Nitrate sensing by the maize root apex transition zone: A merged transcriptomic and proteomic survey

Nitrate sensing by maize root apex transition zone: a merged transcriptomic and proteomic survey

Sara Trevisan[1], Alessandro Manoli[1], Laura Ravazzolo[1], Alessandro Botton[1], Micaela Pivato[1,2], Antonio Masi[1] and Silvia Quaggiotti[1*]

[1]Department of Agriculture, Food, Natural Resources, Animals and Environment (DAFNAE), University of Padova, Agripolis, Viale dell'Università, 16, 35020 Legnaro (PD), Italy

[2]Proteomics Centre of Padova University, VIMM and Padova University Hospital, Via Giuseppe Orus, 2, 35129 Padova, Italy

[*]corresponding author: silvia.quaggiotti@unipd.it

Fax: +39.049.827.2929

sara.trevisan@unipd.it

alessandro.manoli@studenti.unipd.it

laura.ravazzolo.1@gmail.com

alessandro.botton@unipd.it

micaela.pivato@gmail.com

antonio.masi@unipd.it

silvia.quaggiotti@unipd.it

Date of re-submission: 6th March, 2015

Number of pages: 39

Number Figures (colour and black and white figures in print and online): 10

Number of Tables: 3

Supplementary Data: 5

Total word count: 10631

Highlight

A combined untargeted approach was adopted to achieve a picture of the transcriptional and proteomic profiles typifying the maize root transition zone in response to nitrate.

Abstract

Nitrate is an essential nutrient for plants, and crops depend on its availability for growth and development, but its presence in agricultural soils is far to be stable. In order to overcome nitrate fluctuations in soil, plants have developed adaptive mechanisms allowing them to growth despite changes in external nitrate availabilities. Nitrate can act both as nutrient and signal, regulating global gene expression in plants, and the root tip has been proposed as the sensory organ. A set of genome-wide studies evidenced several nitrate-regulated genes in root of many plants, even if only few of them have been carried out on distinct zones of root.

To unravel new details on the transcriptomic and proteomic responses to nitrate availability in a major food crop, a double untargeted approach was conducted on a transition zone enriched root portion of maize seedlings subjected to different nitrate supply.

The results highlighted a complex transcriptomic and proteomic re-programming that occurs in response to nitrate, emphasizing the role of this root zone in sensing and transducing nitrate signal. Our finding inferred the nitrate relationship with biosynthesis and signalling of several phytohormones, such as auxin, strigolactones and brassinosteroids. Moreover, the already hypothesized involvement of nitric oxide in the early response to nitrate was confirmed with the use of nitric oxide inhibitors. Results therein reported also suggest that cytoskeleton activation and cell wall modification occurred in response to nitrate provision in the transition zone.

Key words :

Zea mays L., nitrate, root transition zone, RNA-Seq, iTRAQ, nitric oxide

INTRODUCTION

Nitrogen (N) is one of the most important minerals affecting plant growth, development and production. In aerobic soils, nitrate is the major source of nitrogen for most plant species (Wang YY *et al*., 2012). Its concentration in the soil fluctuates in time and space (Barber, 1995), thus, when soil N is lacking, N fertiliser applications have to sustain crop cultivation (Hirel *et al*., 2007; Robertson and Vitousek, 2009). The incorporation of N into crops is relatively inefficient, with almost 50% of applied nitrogen being utilized (Raun and Johnson, 1999; Hodge *et al*., 2000; Glass, 2003). Therefore, public concerns regarding N leaching from agricultural lands to water resources have increased (Tilman *et al*., 2002; Kant *et al*., 2011). Exceeding nitrate concentrations in drinking water may pose risks to young animals and human health, and a potential cancer risk from nitrate and nitrite in water and food has been reported (Weitzberg and Lundberg, 2013).

Nowadays, in a context of both economic depression and severe environmental law restrictions, farmers have to limit the inputs in crops, although both high productivity and products quality are still required (Dong *et al.*, 2004). Therefore, explaining how the plants cope with their limited resources represents a significant challenge, in order to improve Nitrogen Use Efficiency. Plants respond to limiting nitrogen through a complex of physiological, morphological, and developmental responses. A wide set of papers demonstrated that up to 10% of the Arabidopsis genome (Canales *et al*., 2014) and approximately 7% of the maize transcriptome are nitrogen responsive (Yang *et al*., 2011).

NO_3^- is known to be a dual-function molecule for many plants, being both the major N source and a signalling molecule (Wang YY *et al*., 2012), inducing changes in transcriptome and proteome, thus controlling many aspects of metabolism and development (Krouk *et al*., 2010a; Prinsi *et al*., 2009; Ho *et al*., 2009; Vidal and Gutierrez, 2008; Bouguyon *et al*., 2012; Wang X *et al*., 2012; Vidal *et al*., 2013). The molecular mechanisms by which plants react to nitrate fluctuations are complex and could have a great impact on root development. Cellular profiling of five Arabidopsis root cell types allowed to demonstrate that the nitrogen induced root developmental plasticity is greatly cell-specific and finely regulated within the root (Gifford *et al*., 2008).

The organ devoted to explore regions of the soil is the root and the root apex seems to function as a dynamic sensor of external environment (Baluška *et al*., 2013). The root apex structure consists of a distinct zonation, which is comprised of a meristem, and a zone of rapid cell elongation separated by a transition zone (reviewed in Baluška *et al*., 2010). Transition zone (TZ) has been demonstrated to combine endogenous (hormonal) and/or exogenous (sensorial)

stimuli, functioning as a sensory centre able to re-elaborate information from the external environment in a developmental response (reviewed in Baluška *et al*., 2010). Cells of the TZ were demonstrated to be very sensitive to touch and extracellular calcium (Ishikawa and Evans, 1992; Baluška *et al*., 1996), gravity (Masi *et al*., 2015), auxin (Mugnai *et al*., 2014), osmotic stress (Baluška *et al*., 2013), aluminium (Marciano *et al*., 2010; Sivaguru *et al*., 2013; Yang *et al*., 2014) and oxidative stress (Mugnai *et al*., 2014). Moreover, the TZ has received much attention in studies devoted to the action of hormones (Muraro *et al*., 2013; Moubayidin *et al*., 2013; Takatsuka and Umeda, 2014). Recently, Manoli *et al*. (2014) demonstrated that the control of NO homeostasis occurring in maize root after nitrate perception takes preferentially place at the level of the TZ and that this mechanism could be involved in the regulation of root growth by nitrate. Cell sorting whole-genome approach led to the discovery of highly localized and cell-specific nitrogen responses (Gifford *et al*., 2008), but only few information about specific interaction between nitrate and cells of the transition zone is yet available.

Because of the importance of maize as one of the most worldwide cultivated cereal crops, several studies, mainly based on microarray technology, have monitored the genome-wide transcriptional changes occurring in this species in response to fluctuating NO_3^- concentrations (Liu *et al*., 2008; Trevisan *et al*., 2011; 2012a,b; Xu *et al*., 2011; Zhao *et al*., 2013; Zamboni *et al*., 2014).

Recently, the RNA-Seq strategy has become a useful tool to provide high resolution and detailed information on the transcriptional regulation of genes expression (Martin *et al*., 2013; Vidal *et al*., 2013).

In this work a transcriptome analysis using RNA-Seq technology was assessed to compare gene expression profiles in a transition zone enriched segment of maize root exposed to short-term nitrate treatments.

To complement this study, proteome variations were also investigated through iTRAQ (isobaric tag for relative and absolute quantitation) (Wiese *et al*., 2007) a gel-free, mass spectrometry quantitative technique.

Our results globally provided evidence of the specific role played by this root domain in the nitrate response. Furthermore, an unequivocal contribution of nitric oxide to the nitrate induced transcriptional response in the TZ was postulated. However, findings therein reported pointed out also the existence of NO-independent signalling pathways, which seem to depend both on nitrate itself or on some nitrate assimilation products other than nitric oxide.

MATERIALS AND METHODS

Growth of maize seedlings

Seeds of maize inbred line B73 were sown and then transferred, after germination, to nutrient solution as described by Manoli *et al*. (2014).

In order to evaluate the expression of selected genes in four different portions of roots after nitrate provision, roots of four days seedlings were harvested after 2h of nitrate supply/depletion and the four fragments were immediately cut and frozen (−80 °C), for both the treatment ($+NO_3^-$) and the negative control ($-NO_3^-$). The four zones sampled were: 1- meristem enriched zone (<3mm from the root tip), 2- transition zone enriched portion (<the next 0.8 cm), 3- elongation zone enriched portion (<the next 0.8 cm), and 4- maturation zone (the residual portion). For RNA-Seq and proteomic analyses, the zone 2 from two independent biological replicates was processed. For qPCR analyses three or five independent replicates were utilized and the study was extended to the other three root portions (1, 3, 4) and on seedlings treated with 1mM sodium tungstate dehydrate ($Na_2WO_4.2H_2O$) and 1mM 2-(4-carboxyphenyl)- 4,4,5,5-tetramethylimidazoline-1-oxyl-3-oxide (cPTIO) (Manoli *et al*., 2014), to further investigate the role of NO (for details see specific paragraphs).

mRNA-Seq and bioinformatic analyses

Total RNA was extracted using the TRIzol reagent (Invitrogen, San Giuliano Milanese, Italy). The poly-A mRNAs were purified with the Agencourt AMPure XP beads kit (Beckman Coulter, Inc. Beverly, MA, USA) from two micrograms of total RNA (R.I.N. > 7), fragmented 3 minutes at 94°C, and used for library preparation with the mRNA-Seq Sample Prep kit v2.0 (Illumina, San Diego, CA, USA). Single-read sequencing was carried out on the HiSeq2000 machine (Illumina, San Diego, CA, USA) at the IGA Technology Services (Udine). Base calling was performed using the Illumina Pipeline and sequences were trimmed with ERNE (Vezzi *et al*., 2012). TopHat (Trapnell *et al*., 2012) was used to map and annotate the sequences on the B73 reference genome (ZmB73_RefGen_v2) (Schnable *et al*., 2009) and Cufflinks software (Trapnell *et al*., 2012) for the analysis of differentially expressed genes. Cuffmerge allowed to create a single unified assembly from each individual Cufflinks assemblies. Transcripts with a false discovery rate (FDR) ≤ 0.05 were taken as the highly significant DEGs.

For details and additional information: http://tophat.cbcb.umd.edu/manual.shtml#toph and http://cufflinks.cbcb.umd.edu/manual.html#cuffdiff_output

Chromosome localization of differentially expressed genes

Physical position of genes with a statistically significant differential expression ($p \leq 0.01$) was determined according to the coordinates listed in the GFF file available at the Phytozome database (http://www.phytozome.net/maize.php). Only genes that were included with a mobile window of 21 Mbp containing at least 10 genes were visualized in the map. Charts were generated with Microsoft Excel 2011 for Mac (v 14.4.4).

RNA extraction, cDNA synthesis and qRT−PCR analysis

Total RNA was extracted using the TRIzol reagent (Invitrogen, San Giuliano Milanese, Italy), as indicated by Trevisan *et al*. (2011). Five hundred nanograms of total RNA was pre-treated with RQ1 RNAse-free DNAse (Promega, Milano, Italy) (Falchi *et al*., 2010) and reverse-transcribed to cDNA, as described by Manoli *et al*. (2014).

Primer sequences for the selected genes are listed in Supplementary Table S1. Primers were designed with Primer3 web tool (version 0.4.0; http://frodo.wi.mit.edu/primer3/; Rozen and Skaletsky, 2000) and further verified with PRATO web tool (Nonis *et al*., 2011; http://prato.daapv.unipd.it).

Relative quantification of transcripts by RT-qPCR was performed in a StepOne Real-Time PCR System (Applied Biosystems, Monza, Italy) as described by Nonis *et al*. (2007). Reactions were performed using SYBR Green chemistry (Applied Biosystems, Monza, Italy), following the manufacturer's instructions. Retrotranscribed RNA (2.5ng) was used as template in each reaction as indicated in Trevisan *et al*. (2011). Melting curve analysis confirmed the absence of multiple products and primer dimers. Data were exported and analysed according to Livak and Schmittgen (2001) method using the membrane protein PB1A10.07c (*MEP*, GRMZM2G018103) as reference gene (Manoli *et al*., 2012).

Promoter analyses

Cis-regulatory motifs were identified in the promoter regions of selected genes by Promzea (http://promzea.org, Liseron-Monfils *et al*., 2013). 1000 bp upstream from the predicted transcription start site were analyzed and the common predicted motifs were compared to known promoter motifs in the AthaMap database (Bülow *et al*., 2009) using STAMP (Mahony and Benos, 2007).

Protein Extraction and in situ Trypsin digestion

iTRAQ analysis was carried out as previously described by Tolin *et al*., (2013), with minor changes. Total root proteins were extracted and 70 µg protein samples were loaded into a precast 4-1 2% SDS gel. Single bands were excised, washed with 50mM TEAB

(triethylammoniumbicarbonate), and dried under vacuum after dehydration with acetonitrile. Cysteines were reduced with 10mM dithiothreitol in 50 mM TEAB (1h, 56 °C) and alkylated with 55mM iodoacetamide for 45min at room temperature in the dark. Gel pieces were washed with 50mM TEAB and acetonitrile and dried. Proteins were *in situ* digested with sequencing grade modified trypsin (Promega, Madison, WI, USA) at 37 °C overnight (12.5 $ng \cdot \mu l^{-1}$ trypsin in 50mM TEAB). The obtained peptides were extracted 3 times with 50 µl of 50% acetonitrile in water. 1 µg of each sample was withdrawn and analyzed by LC-MS/MS to check the digestion efficiency. The remaining peptide solution was dried under vacuum.

iTRAQ labeling, strong cation exchange peptide fractionation and LC-MS/MS analysis

Peptides were labelled with iTRAQ reagents (AB Sciex Inc., USA) according to the manufacturer's instructions. Two replications for each condition were labelled with the iTRAQ tags (114, 115 for N supplied, and 116, 117 for N deprived samples, respectively). Samples were separately analyzed by LC-MS/MS. Labelled peptides were vacuum-concentrated, fractionated and subjected to MS-analyses.

The raw LC-MS/MS files were analyzed using Proteome Discoverer 1.4 (Thermo Fisher Scientific), connected to a Mascot Search Engine server (Matrix Science, London, UK). The spectra were searched against a *Zea mays* L. protein database (Sun *et al*., 2009) (http://ppdb.tc.cornell.edu/). FDR were calculated by the Proteome Discoverer. MS/MS spectra containing less than 5 peaks or with a total ion count below 50 were excluded. Only proteins that were identified in all three independent experiments were considered. The quantification was performed normalizing the results on the median value of all measured iTRAQ reporter ratios. A fold change (treated to control) ≥ 1.3 or ≤ 0.77 indicated an increased or decreased protein respectively.

Gene/protein annotation and enrichment analyses

DEGs and proteins were annotated with gene ontology (GO) terms according to the annotation file available at the Phytozome database (http://www.phytozome.net/maize.php). Enrichment analyses for both transcripts and proteins were performed with the Blast2GO software (www.blast2go.org; Conesa *et al*., 2005; Conesa and Gotz, 2008; Gotz *et al*., 2008; Gotz *et al*., 2011) using the overall annotation as a reference and with FDR ≤ 0.05.

To get an improved functional annotation, the protein domains present in the DEGs ($p \leq 0.01$) were clustered according to the InterPro database (Hunter *et al.,* 2012) by PLAZA 3.0 (Proost *et al*., 2015).

RESULTS

Reads processing, transcriptome *de novo* assembly and evaluation

RNA-Seq was used to generate the transcriptomic profiles of the early response to NO_3^- in the selected portion of root (2). Nitrate depleted (24 h) roots were provided with 1 mM NO_3^- for 2 h and compared with nitrate starved roots of the same age. After removal of low quality and contaminated reads, RNA-Seq revealed 158 Mbp raw reads, ranging from 65 to 26 M per sample (Tab. 1). For each set of conditions, more than 80% quality-evaluated reads were mapped to the maize genome sequence. Cufflinks was then used to assemble the aligned reads into transcripts and estimate their abundance to analyse differential expression (Trapnell *et al*., 2010). A total of 109882 transcripts were expressed in the two theses. Among the transcripts detected (RPKM > 0), 154 were significantly responsive to NO_3^- (p-values $\leq$ 0.01, FDR $\leq$ 0.05). Other 524 transcripts were classified as differentially regulated by NO_3^-, but their significance range was less stringent (p-values $\leq$ 0.01, FDR > 0.05). These groups were used to dissect the transcriptional responses associated with the nitrate treatment. Genes are listed in Supplementary Table S2. Of 154 genes (p-values $\leq$ 0.01, FDR $\leq$ 0.05), 111 were up-regulated (72%), while 43 were down-regulated (28%). Among the up-regulated genes, 16 DEGs (13%) were classified as transposable elements and 34 (21%) as uncharacterized proteins.

A considerable part of the differentially expressed transcripts had fold changes greater than 30 (8%), but the largest amount of them showed a 3 to 30 fold change induction (46%) (Fig. 1). The transcription levels of 24% of the down-regulated genes, showed a fold change comprised between 0.3 - 0.1, and the 4% lower than 0.1 (Fig. 1).

Annotation and classification of differentially expressed genes into functional categories

To further characterize the transcriptome response to nitrate, a gene ontology (GO) analysis was carried out on DEGs identified by RNA-Seq ($p \leq 0.01$) (Fig. 2). 86% of the DEGs were successfully classified into the three main GO categories: cellular component, biological process, and molecular function. In the first category, the largest groups were ‘cell part’, ‘membrane-bounded organelle’, ‘membrane part’. Among the biological process subcategories, ‘organic substance metabolic process’, ‘primary metabolic process’, and ‘single-organism metabolic process’ were dominant. In the third classification, the most recurrent term was ‘heme binding’, followed by ‘nucleotide binding’ and ‘metal ion binding’. Almost 7% of the DEGs were annotated as peroxidases, and the 4% had a kinase activity. This classification was confirmed by a domain clustering of the isolated DEGs ($p \leq 0.01$) according to the InterPro database (Supplementary Table S3). A single or more protein domains were found in the 86% of the

accession analyzed, resulting in a total of 1365 isolated domains. The largest groups were related to peroxidases and kinases. Several domains belonging to transcription factor protein families and DNA binding proteins were found (CCAAT-binding transcription factor; zinc finger; bHLH; GRAS; MADS-box; NAC domain; Homeobox domain; AP2/ERF domain; Myb domain; Armadillo-type fold).

The remaining accessions showed interesting protein domains, such as LRR, Hsp family, ABC transporter-like, MFS, AAA+ ATPase, Auxin-induced protein, Aux/IAA-ARF, LEA, LOB, DREPP and t-SNARE. As shown by GO analysis, a large part of the protein domains identified were related to 'oxidation-reduction process' (oxidoreductases, peroxidases, multicopper oxidase, cytochrome P450, alcohol dehydrogenases, carotenoid oxygenases, light-dependent protochlorophyllide reductases, uroporphyrin-III C-methyltransferases).

An enrichment analysis was performed to discover significantly overrepresented functional categories according to two major GO functional domains (biological processes and molecular function; Fig. 3). This analysis was performed only on DEGs with $p \leq 0.01$ and FDR ≤ 0.05. Five GO terms related to biological processes ('response to stress', 'response to oxidative stress', 'oxidation-reduction process', 'response to stimulus', and 'single-organism metabolic process') were significantly over-represented among both up- and down- regulated genes in response to N treatments. Considering the molecular functions, the enriched terms were 'heme binding', 'tetrapyrrole binding', 'oxidoreductase activity', 'peroxidase activity' and 'antioxidant activity'.

Chromosomal localization of genes differentially responding to nitrate treatment

To define the genomic distribution of the DEGs, their chromosomal position was determined (Fig. 4A, B). This analysis revealed an overall distribution of the DEGs on the ten chromosomes, with a gene density *per* chromosome ranging from 6.7% to 16.1% (Fig. 4B). The highest density was observed on chromosome 1, and the lowest on chromosome 9, but chromosomes 3 and 7 had the largest clusters of DEGs.

Validation of sequencing data by qRT-PCR

The expression levels of 41 nitrate-regulated transcripts were further analysed by qPCR to examine the reliability of the observed changes between treatments. Genes were randomly selected according to both their transcription profiles and their putative functions. The transcript levels were measured both on a sample obtained by roots harvested together with those used for the RNA-Seq analysis (technical repetition) and on samples extracted from five other independent biological replicates. The list of 41 genes together with their expression profiles and the results of qRT-PCR validation are included in Supplementary Table S4.

Since only two biological replicates were utilized for RNA-Seq, a number of both false positives and negatives is expected. Therefore, 11 of the 41 transcripts selected for validation were chosen among those differential but less significant ($p \leq 0.01$ and FDR > 0.05 or $p > 0.01$, for details see Supplementary Table S2). Six transcripts belonging all to those characterized by a p value ≤ 0.01 and a FDR ≤ 0.05 were not confirmed by qPCR analysis. On the contrary, all the 11 selected for validation among the differential but not significant ($p \leq 0.01$, FDR > 0.05), were fully confirmed by qPCR analysis on five independent biological repetitions. These results suggest that the number of differential transcripts could be higher than Cufflinks analysis predictions, possibly due to the low number of biological replicates utilised for RNA-Seq.

The comparison among the transcripts accumulation measured for each of 41 genes by RNA-Seq analysis (A), qPCR on RNA derived from the same plants used for RNA-Seq (B), and on other five independent biological replicates (C) is shown in Fig. 5.

The set of genes chosen among the RNA-Seq output list includes also five already identified genes (Trevisan *et al*., 2011), which are expressed in the cells of transition zone in response to nitrate supply (*NR, HB1, HB2, NiR, NRT2.1,* Manoli *et al*., 2014). In the present study all of them showed a strong induction of expression in response to nitrate provision (2 h, 1 mM), fully confirming our previous results and thus supporting the reliability of the experimental design therein adopted.

As a whole qPCR results confirmed the RNA-Seq profiles (except for six false positives), even if the entity of their fluctuations varied with respect to RNA-Seq data. This may be due to the different sensitivity of RNA-Seq analysis and global normalization methods utilized and/or to the low precision of the average values obtained from two biological repetitions.

Among the 35 transcripts which were validated by qPCR, 31 were up-regulated and only four were down-expressed in response to nitrate.

Nitrate differently affects the regulation of gene expression in the four root portions

To evaluate the specificity of the response of the maize root TZ (zone 2) to nitrate, the expression of the 35 transcripts previously selected was also assessed on the other three zones of root (1, 3, 4), both in nitrate-depleted seedlings and after 2h of nitrate provision.

The five genes encoding NR, HB1, HB2, NiR and NRT2.1 which belong to the list of 35 validated transcripts are already known as nitrate responsive genes specifically regulated in the TZ (Manoli *et al*., 2014; Trevisan *et al*., 2014). The present study fully confirmed this finding for all five genes (25, 28, 30, 33, 34), which showed a prominent transcriptional responsiveness to nitrate in the zone 2.

The profile of expression of all 35 genes upon 2 h of nitrate supply (1 mM) in the four different portions of root is shown in Fig. 6. Even if variable and specific profiles were detected, the majority of the up-regulated genes displayed a similar behaviour, with the maximum extent of transcription induction in the zone 2 (TZ enriched) in comparison to the other three zones. Few exceptions are represented by genes showing an high induction of transcription in all the four zones, being thus more transversally regulated by nitrate along the entire root (i.e. transcripts 9, 19, 20, 21, 24, 27).

Independently from the absolute increases/decreases of transcript accumulation, by observing the percentage of mRNAs distribution along root, a widespread transcripts re-localization is clearly appreciable in the TZ enriched portion upon nitrate provision for the majority of the up-regulated genes (Fig. 7). 26 over 35 analysed genes showed the maximum extent of transcription induction or repression in portion 2.

In few cases the increment observed in zone 2 was associated to a clear decrease of the percentage of mRNA abundance in all the other three zones (for details see Fig. 7B).

Tungstate and cPTIO differently affect the gene expression of selected genes

Previous results (Manoli *et al.*, 2014) allowed to hypothesize a NO-dependent signalling pathway controlling the root growth response to nitrate.

To better characterize the putative role of NO signalling on the global transcriptomic response of maize root to nitrate, additional treatments with tungstate and cPTIO were here performed and the level of expression of the 35 selected genes in the TZ-enriched zone was evaluated.

25 over the 35 genes showed a significant decrease of transcription when tungstate was supplied together with nitrate (Fig. 8A, B). Being tungstate a nitrate reductase (NR) inhibitor, results indicate that these genes do not directly respond to nitrate itself, but their regulation rely on some nitrate assimilation products. Furthermore, among those, 15 were also clearly inhibited when a NO scavenger (cPTIO) was applied, allowing to hypothesize a dependency of their transcription by the NO produced by NR.

The transcription of the ten genes ranking in the sub-groups C and D showed an increase of mRNA accumulation in the presence of tungstate, thus suggesting a direct regulation of their transcription by nitrate itself. However, six of them (Fig. 8D) also displayed a slight repression of their expression when cPTIO was supplied with nitrate. This seems to indicate that genes grouped in Fig. 8D, besides being regulated by nitrate itself, are also induced by NO not derived from NR (which in this experiment was repressed by tungstate).

The promoter regions of genes ranking in the four clusters (Fig. 8A,B,C,D) were screened for common *cis*-acting promoter elements, including transcription factor-binding sites (TFBSs), using Promzea (Liseron-Monfils *et al*., 2013).

In silico analysis of 1000 bp upstream the start codons of the co-regulated genes revealed that group-specific binding sites may be attributed to each group (Table 2). For example, genes belonging to group A shared octopine synthase gene (*OCS*) elements and *ARR1*, whereas *TGA1* was characteristic of group B transcripts. *ACE* and *LTRE* characterized the genes of group C and *EIN3*, *EIL1*, *ARF* binding sites were prevalently identified in the promoters of genes clustering in group D. Besides specific motifs, other shared TFBSs, such as WRKY, ABRE, DRE, MADS-sites were found in promoter regions of almost all the four gene clusters.

Proteomic analysis

To complement the transcriptome study a comparative iTRAQ-based proteome survey was performed on TZ-enriched segments after 2 h treatments. Within this time frame, variations in a limited group of proteins was detectable, which can be referred to the early response to nitrate. 880 accessions were identified by merging data obtained from two biological replicates (4179 unique peptides; Supplementary Table S5). The comparison between nitrate supplied and nitrate starved seedlings identified 107 differential expressed proteins. Among them, 41 proteins were up-regulated (fold change ≥1.3), five of which with a fold change ≥ 1.5, and 65 were down-regulated (fold change ≤ 0.77), 21 of which with a fold change ≤ 0.67 (Table 3).

While the number of differentially expressed proteins is similar to that of nitrate-regulated transcripts, the overlap between changes in the proteome and transcriptome is remarkably small (20%). Out of 154 transcripts that changed in abundance after nitrate provision, only 21 of the encoded proteins were found to be differentially expressed.

To further investigate the relationship between modifications in transcript levels and proteins expression changes, a GO enrichment analysis was carried out on the iTRAQ isolated proteins (Fig. 9). Results showed an evident conservation with the RNA-Seq GO enrichment terms, evidencing, also in this case, an high presence of GO terms linked to oxidative stress (response to oxidative stress; oxidoreductase activity; peroxidase activity).

Discussion

High throughput sequencing approaches have become powerful tools to investigate the transcriptomes response to several abiotic stresses (Martin *et al*., 2013). However, as also reported by Gifford *et al*., (2008), in most studies a number of transcripts risks to be excluded,

because they might represent cell specific transcripts whose expression is diluted when considering the whole tissue. In the last years the precise transcriptomic analysis of specific cell types has demonstrated the importance of the cell-specific component in the transcriptional response, that lead to diverse functional competence of the cells (Birnbaum *et al*., 2003; Brady *et al*., 2007; Gifford *et al*., 2008). However a punctual transcriptomic analysis of the root transition zone (TZ) is still missing.

In this study, by using comparative Illumina-based transcriptomic and iTRAQ-based proteomic approaches, putative genes, proteins and pathways possibly responsible for early events controlling nitrate sensing and signalling in the *Zea mays* L. root TZ have been identified.

The statistical analysis ($p \leq 0.01$, FDR ≤ 0.05) revealed a differential mRNAs accumulation for a quite restricted group of transcripts (154 DEGs). Boasting RNA-Seq a general high level of data reproducibility (Marioni *et al*., 2008), the DEGs selection was also enlarged to accessions characterized by a less significant *ratio* between the two treatments ($p \leq 0.01$), to widen the range of information retrievable from the experimental design, avoiding the exclusion of some crucial component of this signalling. This enabled the identification of more than 600 genes putatively responsive to short-term nitrate treatments.

Most of the differentially expressed genes were up-regulated, in accordance with other studies mainly conducted on Arabidopsis and greatly summarized in a recent review by Canales and co-authors (Canales *et al*., 2014). The starvation pre-treatment could probably turn off the expression of many genes related to nitrate assimilation, signalling, and transport, which are then switched on by the nitrate supply (Canales *et al*., 2014).

The GO enriched categories therein evidenced did not include the most consistent GO terms identified by Canales group, which analysed and integrated publicly available Arabidopsis root microarray data, probably because nitrate regulation of gene expression largely depends on the experimental context (Gutiérrez *et al*., 2007; Krouk *et al*., 2010a,b), and thus on the type of root cells analysed, confirming that cell sorting uncover whole-genome responses to nitrate that are missed in whole-root studies (Gifford *et al*., 2008). Moreover functional annotations available for maize (48%) are less abundant and specific than those related to Arabidopsis (91%) (Yi *et al*., 2013). However, considering the single annotations, a great set of genes (i.e. encoding LOB domain-containing proteins, Glucose-6-phosphate dehydrogenase 3, Urophorphyrin methylase 1, Nitrite reductase 1, cytochrome P450, hemoglobin and nitrate transporter 2.1 and others) listed by Canales as the top 50 most consistent and conserved genes in response to nitrate, was here identified, indicating a clear overlap between Arabidopsis and maize.

Moreover, both proteomic and transcriptomic analyses recognised a number of "sentinel target" for primary nitrate response such as ferredoxin and 6-phosphogluconate dehydrogenase (Medici and Krouk, 2014).

To support RNA-Seq results, qPCR validation was performed on arbitrarily chosen transcripts. A high degree (35 of the 41) of result reproducibility was recorded for transcripts selected among both the most significant ones (FDR ≤ 0.05) and those ranking in the less strict group ($p \leq 0.01$), thus confirming the high reliability of RNA-Seq approach.

All of them showed a prevalent transcriptional regulation in the TZ-enriched root portion (2), with some being more strongly (or exclusively) induced in this zone, whilst others more transversally regulated also in other root portions (1, 3, 4). Overall, results suggested the existence of individual and peculiar transcriptional profiles of the maize TZ cells in response to nitrate. This could derive by a different regulation of transcription, but also by a different time lapse of mRNA persistence which might entail a broad re-localization of transcripts along root.

Enriched biological processes related to the most significantly DEGs (FDR ≤ 0.05) included GO-terms associated to peroxidase activity. Peroxidases are encoded by a large multigenic family, and are involved in a wide range of physiological processes all along the plant life cycle such as root elongation regulation through the fine-tuning of the H_2O_2 level (Kawaoka *et al*., 2003; Passardi *et al*., 2005; 2006; Dunand *et al*. 2007). Peroxidases are also part of the heme binding proteins, which are the most representative enriched GO term. It comprises all proteins interacting selectively and non-covalently with heme, such as, beside peroxidases, nitrite and nitrate reductases, flavonoid 3-monooxygenases, cytochrome P450 superfamily proteins and haemoglobins. In general GO enrichment analysis showed that a short term nitrate treatment induced the differential regulation of genes annotated as ROS-related. A number of predicted oxidative stress response enzymes, such as peroxidases were also identified by iTRAQ. These findings, beside supporting the already known participation of ROS in nutritional responses (Shin *et al*., 2005; Krapp *et al*., 2011), also suggest that their localization in maize TZ cells might represent a crucial event for nitrate perception, as already demonstrated in the case of the response to hypoxia (Mugnai *et al*., 2012),

To further characterize the potential physiological impact of the nitrate regulated transcriptomic response, DEGs sequence domains were classified against the InterPro database, thus revealing the presence of several groups of accessions as for example transcription factors (TFs), membranes transporters, protein kinases, DREPP proteins and again cytochromes P450 and peroxidases. Only a restrict group of TFs have been demonstrated to be directly implicated in regulating nitrate responses (Gutiérrez, 2012). TFs known to regulate root development, cell proliferation and elongation, such as ANR1 or HSP, MYB, ERF and LOB-domain (LBD)

members are here demonstrated to be differentially regulated and specifically expressed in the TZ. LBDs affect meristem activity, organ identity, growth, and differentiation and are required for PINs expression, thus regulating auxin transport in roots (Rast *et al*., 2012). Moreover, they have been reported to fine-tune the magnitude of the N response *in planta* by regulating a wide number of N-responsive genes and key transcripts for NO_3^- assimilation (Rubin *et al*., 2009; Yanagisawa, 2014).

Cytochromes P450 superfamily (*CYP*) encodes a large and diverse group of enzymes containing a heme cofactor. These hemeproteins fulfil various biological functions through thousands of catalytic types, including reduction of nitric oxide to nitrous oxide and were recently demonstrated to participate in hormones biosynthesis. Three genes belonging to this family and orthologs to the Arabidopsis *Max1*, *Max3* and *Max4* which are involved in strigolactone (SL) biosynthesis (Zhang *et al*., 2014; Umehara *et al*., 2008; Gomez-Roldan *et al*., 2008), were clearly down regulated by nitrate provision in the maize TZ enriched segment. The same pattern of expression was observed for a gene encoding a PDR protein, that may function as a cellular SLs exporter facilitating delivery of SLs to their site of action (Kretzschmar *et al*., 2012).

Furthermore, SL application was recently shown to reduce plasma membrane levels of PIN1 by enhancing clathrin-mediated endocytosis (Crawford *et al*., 2010; Shinohara *et al*., 2013). Proteome analyses here performed revealed the down regulation of AP-2, a protein involved in clathrin-mediated endocytosis for the regulation of IAA signalling and transport in plants (Yamaoka *et al*., 2013). These results confirm the existence of overlaps between auxin and SL action (Cheng *et al*., 2013) and the involvement of SLs in the nitrate response (Sun *et al*., 2014; Yoneyama *et al*., 2014), but also strengthen the already hypothesised importance of TZ cells in the early nitrate signalling in maize root (Manoli *et al*, 2014).

Moreover, the identification of other components of auxin signalling, as for example *AUX/IAA*, *SAUR* genes, POZ and TAZ domain-containing proteins, and an ortholog of *LCR69* or *LCR68*, corroborate the participation of this hormone in the root response to nitrate (Vidal *et al*., 2010).

Besides auxin and SL, also BRs seem to belong to the network of events involved in the adaptation to nitrate fluctuations. The induction of the transcription of a gene encoding a BR receptor, *BRI1* (*Brassinosteroid-insensitive* 1), already demonstrated by Trevisan *et al*. (2011), was here confirmed. It showed a high extent of down-regulation in the meristem and a strong up-regulation in the TZ, were it seems to be induced in response to a nitrate assimilation product other than NO. Together with *BRI1* the transcript amount of a *BRI1 Associated receptor Kinase 1* (*BAK1*) also increased in the TZ of nitrate-supplied roots.

Furthermore, our data clearly confirm the already hypothesized involvement of nitrate reductase and ns-hemoglobins in the early nitrate sensing by maize roots. Elhiti *et al*., (2013) suggested

that class–2 non-symbiotic hemoglobins play a role in regulating the IAA synthesis and the PIN1-mediated transport of auxin by altering the level NO in specific cells. This might suggest that auxin operates downstream NO in the nitrate signalling in TZ cells of maize root.

NO is a bioactive molecule considered a general plant signal being involved in an extremely wide range of physiological events of plant development, immunity and environmental interactions (Yu *et al*., 2014 and references therein). The production of NO by cells of the TZ seems to be also implicated in the pathway regulating the response to hypoxia in this same species (Mugnai *et al*., 2012).

Here, after having confirmed the peculiarity of transcriptional response to nitrate of the TZ cells, the putative involvement of NO in regulating gene expression was also deepened, by using tungstate and cPTIO, which inhibit the NR activity and scavenge NO respectively. The transcripts amount of 25 of the 35 genes was sensitive to tungstate, suggesting that their nitrate induced regulation does not depend on nitrate itself, but by some other nitrate assimilation products downstream the NR activity. Among those, 15 (almost the 50% of the randomly tested genes), being also down-regulated by cPTIO, seem to be induced by NR-derived NO, thus allowing to hypothesise a more generalized NO involvement in the pathway governing the nitrate response in TZ cells. The promoter regions of these NO regulated genes share OCS and ARR1 *cis*-elements that were not identified in the other groups. OCS confer regulation by NO (Palmieri *et al*., 2008), whereas ARR1 are typical citokinin responsive elements (Hwang *et al*., 2012).

A more restrict group (10 on 35) were directly regulated by nitrate itself, even if six of them, would seem also to be NO-responsive. Further experiments are needed to deepen this odd result.

The NO-mediated nitrate regulation of primary root elongation (Manoli *et al.*, 2014; Trevisan *et al.*, 2014) should depend on cytoskeletal rearrangements (Kasprowicz *et al*., 2009). Several cytoskeletal genes were differentially regulated by nitrate supply in the TZ enriched zone. These proteins participate to different plant processes, including establishing cell polarity, determining the location of the division plane, reprogramming of cell wall development and deposition, cell elongation, positioning receptors and transmembrane transport, transporting mRNAs within the cell and positioning the nucleus (reviewed in Smith and Oppenheimer, 2005). An activation of cytoskeleton was demonstrated also by the iTRAQ identification of vesicle-related and DREPP domain-containing proteins, a domain that confers microtubule binding activity (Li *et al*., 2011). Moreover, our data revealed that regulation of several targets related to cell wall deposition, modification and reorganization is affected by nitrate supply, and probably results in an altered root growth (Baluška *et al*., 2003).

However, it must be highlighted that, despite some fascinating information, only the 20% of the protein profiles were supported by the transcriptomic data. A generally low congruency of proteomic and transcriptional profiles has been previously reported (Reviewed in Vogel and Marcotte, 2012). Several factors may cause the small overlap between the two approaches. First, iTRAQ technology might not detect proteins with a low abundance, while RNA-Seq could detect low transcript levels of the corresponding genes (Lan *et al*., 2012).

Moreover, a change in transcript abundance may not be translated soon after into changes in protein level (Rajasundaram *et al*., 2014), suggesting the existence of a lag time between NO_3^--induced transcription and translation. Furthermore, proteins may be synthesized in a specific tissue and then move toward another, as in the case of UPB1, which is implicated in the control of ROS homeostasis along Arabidopsis roots (Tsukagoshi *et al*., 2010). Here the transcription of a gene encoding a maize ortholog of UPB1 was up-regulated by nitrate even if the protein was not included in the iTRAQ output in the same root zone. Furthermore, the existence of miRNA-guided post-transcriptional mechanisms of regulation must be considered. In fact *in situ* hybridization of transcripts for nitrate-responsive maize miRNA revealed their localization in cells of meristem and of the TZ (Trevisan *et al*., 2012a,b).

Before concluding it must be highlighted that 13% of up-regulated DEGs are transposable elements (TEs). Several studies reported TEs overexpression following abiotic or biotic stress in plants (reviewed by Benoît Chénais *et al.*, 2012). Our findings endorse the important role of epigenetic processes also in adaptation to nitrate fluctuations.

To conclude, information obtained from both high-resolution data sets depict a snapshot of genes and proteins participating to the early response to nitrate in the root transition zone (Fig.10). The identification of candidate genes differentially regulated by the presence of nitrate and specifically located in this root zone evidenced the spatial transcriptional complexity that underlies root response to nutritional inputs. TZ was confirmed as a critical zone in sensing nitrate which seems to directly influence the transcript levels for few genes, but also to indirectly act through the NR action. NO was definitely established as a key player in the maize root response to nitrate, but also other nitrate-derived signals seem to contribute to this pathway. Both transcriptomic and proteomic approaches suggested that ROS signalling might play a pivotal role in the complex signalling featuring nitrate perception and leading to the root development tuning, likelihood controlling the balance between cell proliferation and cell elongation thus accomplishing the developmental plasticity which typically characterize this root zone.

Acknowledgements

Funds were provided by the University of Padova (‘ex 60%’: 2012–2013, 2013–2014).

1

References

Baluška F, Barlow PW, Parker JS, Volkmann D. 1996. Symmetric reorganizations of radiating microtubules around pre-mitotic and post-mitotic nuclei of dividing cells organized within intact root meristems. *Journal of Plant Physiology* **149**, 119–128.

Baluška F, Samaj J, Wojtaszek P, Volkmann D, Menzel D. 2003. Cytoskeleton-plasma membrane-cell wall continuum in plants. Emerging links revisited. *Plant Physiology* **133**, 482-491.

Baluška F, Mancuso S, Volkmann D, Barlow PW. 2010. Root apex transition zone: a signalling-response nexus in the root. *Trends in Plant Sciences* **15**, 402-408.

Baluška F, Mancuso S. 2013. Root apex transition zone as oscillatory zone. *Frontiers in Plant Science* **4**, 354.

Barber SA. 1995. Soil Nutrient Bioavailability: A Mechanistic Approach. John Wiley & Sons, 2nd eds. New York, 414.

Birnbaum K, Shasha DE, Wang JY, Jung JW, Lambert GM, Galbraith DW, Benfey PN. 2003. A gene expression map of the Arabidopsis root. *Science* **302**, 1956-1960.

Bouguyon E, Gojon A, Nacry P. 2012. Nitrate sensing and signalling in plants. *Seminars in Cell and Developmental Biology* **23**, 648-654.

Brady SM, Orlando DA, Lee J-Y, Wang JY, Koch J, Dinneny JR, Mace D, Ohler U, Benfey PN. 2007. A high-resolution root spatiotemporal map reveals dominant expression patterns. *Science* **318**, 801.

Bülow L, Engelmann S, Schindler M, Hehl R. 2009. AthaMap, integrating transcriptional and post-transcriptional data. *Nucleic Acids Research* **37**, D983-986.

Canales J, Moyano TC, Villarroel E, Gutiérrez RA. 2014. Systems analysis of transcriptome data provides new hypotheses about Arabidopsis root response to nitrate treatments. *Frontiers in Plant Science* **7**, 5-22.

Chénais B, Caruso A, Hiard S, Casse N. 2012. The impact of transposable elements on eukaryotic genomes: from genome size increase to genetic adaptation to stressful environments. *Gene* **509**, 7-15.

Cheng X, Ruyter-Spira C, Bouwmeester H. 2013. The interaction between strigolactones and other plant hormones in the regulation of plant development. *Frontiers in Plant Science* **4**, 199.

Conesa A, Götz S, García-Gómez JM, Terol J, Talón M, Robles M. 2005. Blast2GO: a universal tool for annotation, visualization and analysis in functional genomics research. *Bioinformatics* **21**, 3674-3676.

Conesa A, Götz S. 2008. Blast2GO: A Comprehensive Suite for Functional Analysis in Plant Genomics. *International Journal of Plant Genomics* **2008,** 1-12.

Crawford S, Shinohara N, Sieberer T, Williamson L, George G, Hepworth J, Müller D, Domagalska MA, Leyser O. 2010. Strigolactones enhance competition between shoot branches by dampening auxin transport. *Development* **137**, 2905-2913.

Dong S, Lailiang C, Carolyn FS, Leslie HF. 2004. N uptake, soil retention and loss of soil-applied 15NH4 15NO3 in young Fuji/M.26 apple trees with different N status. *Journal of Horticultural Science and Biotechnology* **79**, 395–399.

Dunand C, Crèvecoeur M, Penel C. 2007. Distribution of superoxide and hydrogen peroxide in Arabidopsis root and their influence on root development: possible interaction with peroxidases. *New Phytologist* **174**, 332-341.

Elhiti M, Hebelstrup KH, Wang A, Li C, Cui Y, Hill RD, Stasolla C. 2013. Function of type-2 Arabidopsis hemoglobin in the auxin-mediated formation of embryogenic cells during morphogenesis. *The Plant Journal* **74**, 946-958.

Falchi R, Cipriani G, Marrazzo T, Nonis A, Vizzotto G, Ruperti B. 2010. Identification and differential expression dynamics of peach small GTPases encoding genes during fruit development and ripening. *Journal of Experimental Botany* **61**, 2829–2842.

Götz S, García-Gómez JM, Terol J, Williams TD, Nagaraj SH, Nueda MJ, Robles M, Talón M, Dopazo J, Conesa A. 2008. High-throughput functional annotation and data mining with the Blast2GO suite. *Nucleic Acids Research* **36**, 3420-3435.

Götz S, Arnold R, Sebastián-León P, Martín-Rodríguez S, Tischler P, Jehl MA, Dopazo J, Rattei T, Conesa A. 2011. B2G-FAR, a species centered GO annotation repository. *Bioinformatics* **27**, 919-924.

Hirel B, Le Gouis J, Ney B, Gallais A. 2007. The challenge of improving nitrogen use efficiency in crop plants: towards a more central role for genetic variability and quantitative genetics within integrated approaches. *Journal of Experimental Botany* **58**, 2369-2387.

Ho CH, Lin SH, Hu HC, Tsay YF. 2009. CHL1 functions as a nitrate sensor in plants. *Cell* **138**, 1184-1194.

Hodge A, Robinson D, Fitter A. 2000. Are microorganisms more effective than plants at competing for nitrogen? *Trends in Plant Sciences* **5**, 304-308.

Hwang I, Sheen J, Müller B. 2012. Cytokinin signaling networks. *Annual Review of Plant Biology* **63**, 353–380.

Hunter S, Jones P, Mitchell A. 2012. InterPro in 2011: new developments in the family and domain prediction database. *Nucleic Acids Research* **40**, D306–D312.

Kant S, Bi Y-M, Rothstein SJ. 2011. Understanding plant response to nitrogen limitation for the improvement of crop nitrogen use efficiency. *Journal of Experimental Botany* **62**, 1499–1509.

Kasprowicz A, Szuba A, Volkmann D, Baluška F, Wojtaszek P. 2009. Nitric oxide modulates dynamic actin cytoskeleton and vesicle trafficking in a cell type-specific manner in root apices. *Journal of Experimental Botany* **60**, 1605-1617.

Kawaoka A, Matsunaga E, Endo S, Kondo S, Yoshida K, Shinmyo A, Ebinuma H. 2003. Ectopic expression of a horseradish peroxidase enhances growth rate and increases oxidative stress resistance in hybrid aspen. *Plant Physiology* **132**, 1177-1185.

Krapp A, Berthomé R, Orsel M, Mercey-Boutet S, Yu A, Castaings L, Elftieh S, Major H, Renou JP, Daniel-Vedele F. 2011. Arabidopsis roots and shoots show distinct temporal adaptation patterns toward nitrogen starvation. *Plant Physiology* **157**, 1255-1282.

Kretzschmar T, Kohlen W, Sasse J, Borghi L, Schlegel M, Bachelier JB, Reinhardt D, Bours R, Bouwmeester HJ, Martinoia E. 2012. A petunia ABC protein controls strigolactone-dependent symbiotic signalling and branching. *Nature* **483**, 341-344.

Krouk G, Mirowski P, LeCun Y, Shasha DE, Coruzzi GM. 2010a. Predictive network modeling of the high-resolution dynamic plant transcriptome in response to nitrate. *Genome Biology* **11**, R123.

Krouk G, Crawford NM, Coruzzi GM, Tsay YF. 2010b. Nitrate signalling: adaptation to fluctuating environments. *Current Opinion in Plant Biology* **3**, 266-273.

Lan P, Li W, Schmidt W. 2012. Complementary proteome and transcriptome profiling in phosphate-deficient Arabidopsis roots reveals multiple levels of gene regulation. *Molecular and Cell Proteomics* **11**, 1156-1166.

Li J, Wang X, Qin T, Zhang Y, Liu X, Sun J, Zhou Y, Zhu L, Zhang Z, Yuan M, Mao T. 2011. MDP25, a novel calcium regulatory protein, mediates hypocotyl cell elongation by destabilizing cortical microtubules in Arabidopsis. *Plant Cell* **23**, 4411-4427.

Liseron-Monfils C, Lewis T, Ashlock D, McNicholas PD, Fauteux F, Strömvik M, Raizada MN. 2013. Promzea: a pipeline for discovery of co-regulatory motifs in maize and other plant species and its application to the anthocyanin and phlobaphene biosynthetic pathways and the Maize Development Atlas. *BMC Plant Biology* **13**, 42.

Liu J, Han L, Chen F, Bao J, Zhang F, Mi G. 2008. Microarray analysis reveals early responsive genes possibly involved in localized nitrate stimulation of lateral root development in maize (*Zea mays* L.). *Plant Science* **175**, 272-282.

Mahony S, Benos PV. 2007. STAMP: a web tool for exploring DNA-binding motif similarities. *Nucleic Acids Research* **35**, W253-W258.

Manoli A, Begheldo M, Genre A, Lanfranco L, Trevisan S, Quaggiotti S. 2014. NO homeostasis is a key regulator of early nitrate perception and root elongation in maize. *Journal of Experimental Botany* **65**, 185-200.

Manoli A, Sturaro A, Trevisan S, Quaggiotti S, Nonis A. 2012. Evaluation of candidate reference genes for qPCR in maize. *Journal of Plant Physiology* 169, 807–815.

Marioni JC, Mason CE, Mane SM, Stephens M, Gilad Y. 2008. RNA-seq: an assessment of technical reproducibility and comparison with gene expression arrays. *Genome Research* **18**, 1509-1517.

Martin LB, Fei Z, Giovannoni JJ, Rose JK. 2013. Catalyzing plant science research with RNA-seq. *Frontiers in Plant Science* **4**, 66.

Masi E, Ciszak M, Comparini D, Monetti E, Pandolfi C, Azzarello E, Mugnai S, Baluška F, Mancuso S. 2015. The Electrical Network of Maize Root Apex is Gravity Dependent. *Scientific Reports* **5**, 7730.

Medici A, Krouk G. 2014. The Primary Nitrate Response: a multifaceted signalling pathway. *Journal of Experimental Botany* **65**, 5567-5576.

Moubayidin L, Di Mambro R, Sozzani R, et al. 2013. Spatial coordination between stem cell activity and cell differentiation in the root meristem. *Developmental Cell* **26**, 405-15.

Mugnai S, Pandolfi C, Masi E, Azzarello E, Monetti E, Comparini D, Voigt B, Volkmann D, Mancuso S. 2014. Oxidative stress and NO signalling in the root apex as an early response to changes in gravity conditions. *BioMed Research International* **2014**, 1-12.

Mugnai S, Azzarello E, Baluška F, Mancuso S. 2012. Local root apex hypoxia induces NO-mediated hypoxic acclimation of the entire root. *Plant and Cell Physiology* **53**, 912-920.

Muraro D, Byrne H, King J, Bennett M. 2013. The role of auxin and cytokinin signalling in specifying the root architecture of *Arabidopsis thaliana*. *Journal of Theoretical Biology* **317**, 71-86.

Nonis A, Ruperti B, Falchi R, Casatta E, Thamashebi SE, Vizzotto G. 2007. Differential expression and regulation of a neutral invertase encoding gene from peach (*Prunus persica*): evidence for a role in fruit development. *Physiologia Plantarum* **129**, 436–446.

Nonis A, Scortegagna M, Nonis A, Ruperti B. 2011. PRaTo: a web-tool to select optimal primer pairs for qPCR. *Biochemical and Biophysical Research Communications* **415**, 707–708.

Palmieri MC, Sell S, Huang X, Scherf M, Werner T, Durner J, Lindermayr C. 2008. Nitric oxide-responsive genes and promoters in *Arabidopsis thaliana*: a bioinformatics approach. *Journal of Experimental Botany* **59**, 177-186.

Passardi F, Cosio C, Penel C, Dunand C. 2005. Peroxidases have more functions than a Swiss army knife. *Plant Cell Reports* **24**, 255-265.

Passardi F, Tognolli M, De Meyer M, Penel C, Dunand C. 2006. Two cell wall associated peroxidases from Arabidopsis influence root elongation. *Planta* **223**, 965-974.

Proost S, Van Bel M, Vaneechoutte D, Van de Peer Y, Inzé D, Mueller-Roeber B, Vandepoele K. 2015. PLAZA 3.0: an access point for plant comparative genomics. *Nucleic Acids Research* **43**, D974-D981.

Rajasundaram D, Selbig J, Persson S, Klie S. 2014. Co-ordination and divergence of cell-specific transcription and translation of genes in arabidopsis root cells. *Annals of Botany* **114**, 1109-1123.

Rast MI, Simon R. 2012. Arabidopsis JAGGED LATERAL ORGANS acts with ASYMMETRIC LEAVES2 to coordinate KNOX and PIN expression in shoot and root meristems. *Plant Cell* **24**, 2917-2933.

Raun WR, Johnson GV. 1999. Improving nitrogen use efficiency for cereal production. *Agronomy Journal* **91**, 357-363.

Robertson GP, Vitousek PM. 2009. Nitrogen in agriculture: balancing the cost of an essential resource. *Annual Review of Environment and Resources* **34**, 97–125.

Rubin G, Tohge T, Matsuda F, Saito K, Scheible WR. 2009. Members of the LBD family of transcription factors repress anthocyanin synthesis and affect additional nitrogen responses in Arabidopsis *Plant Cell* **21**, 3567-3584.

Sahu PP, Pandey G, Sharma N, Puranik S, Muthamilarasan M, Prasad M. 2013. *Plant Cell Reports* **32**, 1151-1159.

Schnable PS, Ware D, Fulton RS, et al. 2009. The B73 maize genome: complexity, diversity, and dynamics. *Science* **326**, 1112–1115.

Shin R, Berg RH, Schachtman DP. 2005. Reactive oxygen species and root hairs in Arabidopsis root response to nitrogen, phosphorus and potassium deficiency. *Plant Cell Physiology* **46**, 1350–1357.

Shinohara N, Taylor C, Leyser O. 2013. Strigolactone can promote or inhibit shoot branching by triggering rapid depletion of the auxin efflux protein PIN1 from the plasma membrane. *PLoS Biology* **11**, e1001474.

Sivaguru M, Liu J, Kochian LV. 2013. Targeted expression of SbMATE in the root distal transition zone is responsible for sorghum aluminum resistance. *The Plant Journal* **76**, 297-307.

Smith LG, Oppenheimer DG. 2005. Spatial control of cell expansion by the plant cytoskeleton. *Annual Review of Cell and Developmental Biology* **21**, 271-295.

Sun Q, Zybailov B, Majeran W, Friso G, Olinares PD, van Wijk KJ. 2009. PPDB, the Plant Proteomics Database at Cornell. *Nucleic Acids Research* **37**, D969-974.

Sun H, Tao J, Liu S, Huang S, Chen S, Xie X, Yoneyama K, Zhang Y, Xu G. 2014. Strigolactones are involved in phosphate- and nitrate-deficiency-induced root development and auxin transport in rice. *Journal of Experimental Botany* **65**, 6735-6746.

Takatsuka H, Umeda M. 2014. Hormonal control of cell division and elongation along differentiation trajectories in roots. *Journal of Experimental Botany* **65**, 2633-2643.

Tilman D, Cassman KG, Matson PA, Naylor R, Polasky S. 2002. Agricultural sustainability and intensive production practices. *Nature* **418**, 671–677.

Tolin S, Arrigoni G, Trentin AR, Veljovic-Jovanovic S, Pivato M, Zechman B, Masi A. 2013. Biochemical and quantitative proteomics investigations in Arabidopsis ggt1 mutant leaves reveal a role for the gamma-glutamyl cycle in plant's adaptation to environment. *Proteomics* **13**, 2031-2045.

Trapnell C, Williams BA, Pertea G, Mortazavi A, Kwan G, van Baren MJ, Salzberg SL, Wold BJ, Pachter L. 2010. Transcript assembly and quantification by rna-seq reveals unannotated transcripts and isoform switching during cell differentiation. *Nature Biotechnology* **28**, 511–515.

Trapnell C, Roberts A, Goff L, Pertea G, Kim D, Kelley DR, Pimentel H, Salzberg SL, Rinn JL, Pachter L. 2012. Differential gene and transcript expression analysis of RNA-seq experiments with TopHat and Cufflinks. *Nature Protocols* **7**, 562–578.

Trevisan S, Manoli A, Begheldo M, Nonis A, Enna M, Vaccaro S, Caporale G, Ruperti B, Quaggiotti S. 2011. Transcriptome analysis reveals coordinated spatiotemporal regulation of hemoglobin and nitrate reductase in response to nitrate in maize roots. *New Phytologist* **192**, 338-352.

Trevisan S, Nonis A, Begheldo M, Manoli A, Palme K, Caporale G, Ruperti B, Quaggiotti S. 2012a. Expression and tissue-specific localization of nitrate-responsive miRNAs in roots of maize seedlings. *Plant Cell and Environment* **35**, 1137-1155.

Trevisan S, Begheldo M, Nonis A, Quaggiotti S. 2012b. The miRNA-mediated post-transcriptional regulation of maize response to nitrate. *Plant Signalling and Behavior* **7**, 822-826.

Trevisan S, Manoli A, Quaggiotti S. 2014. NO signalling is a key component of the root growth response to nitrate in *Zea mays* L. *Plant Signalling and Behavior* **9**, e28290.

Tsukagoshi H, Busch W, Benfey PN. 2010. Transcriptional regulation of ROS controls transition from proliferation to differentiation in the root. *Cell* **143**, 606-616.

Umehara M, Hanada A, Yoshida S, et al. 2008. Inhibition of shoot branching by new terpenoid plant hormones *Nature* **455**, 195–200.

Vezzi F, Del Fabbro C, Tomescu AI, Policriti A. 2012. rNA: a fast and accurate short reads numerical aligner. *Bioinformatics* **28**, 123-124.

Vidal EA, Gutiérrez RA. 2008. A systems view of nitrogen nutrient and metabolite responses in Arabidopsis. *Current Opinion in Plant Biology* **11**, 521-529.

Vidal EA, Araus V, Lu C, Parry G, Green PJ, Coruzzi GM, Gutiérrez RA. 2010. Nitrate-responsive miR393/AFB3 regulatory module controls root system architecture in *Arabidopsis thaliana*. *Proceedings Of The National Academy Of Sciences, USA* **107**, 4477–4482.

Vidal EA, Moyano TC, Krouk G, Katari MS, Tanurdzic M, McCombie WR, Coruzzi GM, Gutiérrez RA. 2013. Integrated RNA-seq and sRNA-seq analysis identifies novel nitrate-responsive genes in *Arabidopsis thaliana* roots. *BMC Genomics* **14**, 701.

Vogel C, Marcotte EM. 2012. Insights into the regulation of protein abundance from proteomic and transcriptomic analyses. *Nature Reviews Genetics* **13**, 227-232.

Wang L, Li PH, Brutnell TP. 2010. Exploring plant transcriptomes using ultra high-throughput sequencing. *Briefings in Functional Genomics* **9**,118-128.

Wang X, Bian Y, Cheng K, Zou H, Sun SS, He JX. 2012. A comprehensive differential proteomic study of nitrate deprivation in Arabidopsis reveals complex regulatory networks of plant nitrogen responses. *Journal of Proteome Research* **11**, 2301-2315.

Wang YY, Hsu PK, Tsay YF. 2012. Uptake, allocation and signalling of nitrate. *Trends in Plant Science* **17**, 458–467.

Weitzberg E, Lundberg JO. 2013. Novel aspects of dietary nitrate and human health. *Annual Review of Nutrition* **33**, 129-159.

Wiese S, Reidegeld KA, Meyer HE, Warscheid B. 2007. Protein labeling by iTRAQ: a new tool for quantitative mass spectrometry in proteome research. *Proteomics* **7**, 340-350.

Xu Z, Zhong S, Li X, Li W, Rothstein SJ, Zhang S, Bi Y, Xie C. 2011. Genome-wide identification of microRNAs in response to low nitrate availability in maize leaves and roots. *PLoS ONE* **6**:e28009.

Yamaoka S, Shimono Y, Shirakawa M, Fukao Y, Kawase T, Hatsugai N, Tamura K, Shimada T, Hara-Nishimura I. 2013. Identification and dynamics of Arabidopsis adaptor protein-2 complex and its involvement in floral organ development. *Plant Cell* **25**, 2958-2969.

Yanagisawa S. 2014. Transcription factors involved in controlling the expression of nitrate reductase genes in higher plants. *Plant Science* **229**, 167-171.

Yang XS, Wu J, Ziegler TE, et al. 2011. Gene expression biomarkers provide sensitive indicators of *in planta* nitrogen status in maize. *Plant Physiology* **157**, 1841-1852.

Yang ZB, Geng X, He C, Zhang F, Wang R, Horst WJ, Ding Z. 2014. TAA1-regulated local auxin biosynthesis in the root-apex transition zone mediates the aluminum-induced inhibition of root growth in Arabidopsis. *Plant Cell* **26**, 2889-2904.

Yi X, Du Z, Su Z. 2013. PlantGSEA: a gene set enrichment analysis toolkit for plant community. *Nucleic Acids Research* **41**, W98-103.

Yoneyama K, Kisugi T, Xie X, Arakawa R, Ezawa T, Nomura T, Yoneyama K. 2014. Shoot-derived signals other than auxin are involved in systemic regulation of strigolactone production in roots. *Planta* doi: 10.1007/s00425-014-2208-x.

Yu M, Lamattina L, Spoel SH, Loake GJ. 2014. Nitric oxide function in plant biology: a redox cue in deconvolution. *New Phytologist* **202**, 1142-1156.

Zamboni A, Astolfi S, Zuchi S, Pii Y, Guardini K, Tononi P, Varanini Z. 2014. Nitrate induction triggers different transcriptional changes in a high and a low nitrogen use efficiency maize inbred line. *Journal of Integrative Plant Biology* **56**, 1080-1094.

Zhang Y, van Dijk AD, Scaffidi A, et al. 2014. Rice cytochrome P450 MAX1 homologs catalyze distinct steps in strigolactone biosynthesis. *Nature Chemical Biology* **10**, 1028-1033.

Zhao Y, Xu Z, Mo Q, Zou C, Li W, Xu Y, Xie C. 2013. Combined small RNA and degradome sequencing reveals novel miRNAs and their targets in response to low nitrate availability in maize. *Annals of Botany* **112**, 633-642.

Tables

Table 1. Summary of reads obtained by RNA-Seq analysis. For each thesis two biological replicates were processed (+N sample: libraries 1-2; -N sample: libraries 3-4).

	Libraries							
	1		**2**		**3**		**4**	
No. of total reads	38787677	100%	65608508	100%	26009381	100%	28335261	100%
No. of mapped reads	33537854	86%	57435252	88%	22449519	86%	23561167	83%
Unique	12117740	31%	20536079	31%	8177365	31%	8386919	30%
Multimatch	21420114	55%	36899173	56%	14272154	55%	15174248	54%
No. of reads not mapped	5249823	14%	8173256	12%	3559862	14%	4774094	17%

Table 2. Classification of the *cis*-elements represented in the promoter sequences of the four gene groups characterized by specific gene expressions in response to cPTIO, W and NO_3^- treatments.

***Cis*-element**	**Consensus sequence**	**Description**	**Group**
ARRIAT	NGATT	ARR1-binding element	A
TELO-box	AAACCCTAA	Telomere motif	A
OCS	TGACGYAAGSRMTKACGYMM	octopine synthase gene promoter element	A
HaHB-4		HD-Zip; JA and ET-related	A
TGA1:	TGACGTGG	HD-Zip	B
TEF-box	AGGGGCATAATGGTAA	Telomere motif	B
JASE2	CATACGTCGTCAA	A/C box-like motif	B
BLR-RPL-PNY	AAATTAAA	HomeoDomain	B
TaNAC69	CCNAGGCACG	NAC domain	B
EIN3	GGATTCAAGGGGGCATGTATCTTGAATCC	Ethylene responsive elements	D
EIL1	TTCAAGGGGGCATGTATCTTGAA	Ethylene responsive elements	D
ARF	TGTCTC	Auxin response factors.	D
PREATPRODH	ACTCATCCT	Pro- or hypoosmolarity-responsive element (PRE)	D
ACEAtCHS	GACACGTAGA	ACE promoter motif	C
LTRE	ACCGACA	Putative low temperature responsive element	C
LS7	TCTACGTCAC	bZIP	C
I-BOX	GATAAG	MYB, light regulation	C
DRE	TACCGACAT	Dehydration-responsive element	C
ATHB1	CAATTATTG	HomeoDomain	C
W-box	TTGACT	WRKY	C

Table 3. iTRAQ differentially regulated proteins (indicated by the maize GDB accession ID). Fold changes indicate up-regulated (≥ 1.5) and down-regulated (≤ 0.7) proteins, according to the +N/-N treatment ratio. Accessions present in both RNA-Seq and iTRAQ lists are evidenced in bold case.

Accession	Fold changes	Description
Glycolysis, gluconeogenesis, C-compound and carbohydrate metabolism		
GRMZM5G828229	1.6	Dihydrolipoyl dehydrogenase
GRMZM2G440208	1.5	6-phosphogluconate dehydrogenase
GRMZM2G166767	0.6	RHM1
Nitrogen metabolism, amino acid metabolism and protein/peptide degradation		
GRMZM2G102959	3.9	Ferredoxin--nitrite reductase
GRMZM2G050514	1.7	Glutamine synthetase root isozyme 1
Cell defense		
GRMZM2G051943	0.7	CHIA Endochitinase A
GRMZM2G125893	0.7	Nucleoside diphosphate kinase
GRMZM2G373522	0.5	DHN-2 dehydrin
GRMZM2G108219	0.6	Peroxidase 11
GRMZM2G088765	0.5	Peroxidase 54
GRMZM2G044049	0.5	Similar to Peroxidase
GRMZM2G427937	0.5	Peroxidase
Post-transcriptional and post-translational mechanisms		
GRMZM2G160994	1.7	PPR-like superfamily protein
AC233872.1	0.7	Mitochondrial glycoprotein
GRMZM2G464401	0.7	Plasminogen activator inhibitor 1 RNA-binding protein
GRMZM2G176707	0.6	Nucleosome/chromatin assembly factor group A
GRMZM2G045503	0.6	Similar to RNA-binding protein
GRMZM2G161746	0.6	Trypsin inhibitor heavy chain H3
GRMZM2G116282	0.6	Plasminogen activator inhibitor 1 RNA-binding protein
GRMZM2G157470	0.5	Brain acid soluble protein 1
Cytoskeleton organization/vescicules trafficking		
GRMZM2G071089	0.6	DREPP2
GRMZM2G001514	0.6	Fasciclin-like arabinogalactan protein 7
GRMZM2G137236	0.6	AP-2 complex, alpha subunit
GRMZM2G123558	0.7	DREPP4 protein
Others		
GRMZM2G109130	1.5	Lipoxygenase
GRMZM2G051270	1.5	ATP sulfurylase, sulfurylase 4, chloroplastic
GRMZM2G120876	1.5	Probable mitochondrial import receptor subunit TOM40-2
GRMZM2G358059	0.6	CRT1 Calreticulin
GRMZM2G013461	0.6	CC4 Multidomain cystatin

Figure legends

Fig. 1. Graphic distribution of DEGs identified (FDR ≤ 0.05) by the RNA-Seq analysis from the comparison between transition zone enriched samples of nitrate starved seedlings transferred for 2h in a nitrate supplied (1mM NO_3^-) or depleted (-N, negative control) solution. DEGs were classified in up- (+N/-N>1) and down-regulated (+N/-N<1) according to their RPKM values, and data are reported as percentage in the graphic. Among up and down-regulated groups of transcripts, several ranges of induction or repression are shown.

Fig. 2. Histograms for Gene Ontology (Blast2go) classification of DEGs ($p \leq 0.01$) isolated by RNA-Seq analysis in the three main categories: Cellular Component (A), Biological Process (B) and Molecular Function (C). The x-axis indicates the percentage of the annotations distribution in each category.

Fig. 3. Identification of over-represented GO terms in the DEGs set (FDR ≤ 0.05) by enrichment analysis (Blast2go). The graph represents the percentage of annotated GO (Biological Process and Molecular Function) categories of data set identified which were found to be significantly enriched (FDR ≤ 0.05).

Fig. 4. Physical position (A) and frequency (B) of differentially expressed genes ($p \leq 0.01$) on the ten maize chromosomes. (A) Each chromosome is represented by a vertical grey bar, supported by graphics indicating genetic positions of a subset of DEGs identified by RNA-Seq analysis. Only genes included within a mobile window of 21Mbp containing more than 10 differential transcripts are shown. The number of genes in each region was then converted to a percentage of the total number of genes for the chromosome and graphed (B).

Fig. 5. RNA-Seq profiles validation. Relative expression profiles of the selected 41 genes identified from RNA-Seq analysis (A) were assessed by Real time quantitative PCR in both technical (B) and biological (C) replicates and were herein reported, as relative expressions obtained from +N/-N ratio, according to RPKM values RPKM of each DEG analyzed. Asterisks (* or **) on top of columns indicate the significance of data (no= FDR ≤ 0.05; *= $p \leq 0.01$, FDR > 0.05; **= FDR > 0.05) (A). Error bars represent the standard error of the mean of two technical replicates (B) and five biological replicates (C). Up-regulated genes (+N/-N > 1 according to RNA-Seq analysis) are reported on the left panel, while down regulated (+N/-N<1 relative transcript level according to RNA-Seq analysis) are shown in the right panel. RPKM detected for GRMZM2G015933 in the –N condition was arbitrarily fixed to 0.001 to calculate the +N/-N ratio.

Fig. 6. Heat map representation of qPCR differential relative expression of 35 selected DEGs in 4 sections (1, meristem enriched zone; 2, transition zone enriched portion; 3 elongation zone

enriched portion; 4, maturation zone enriched portion) of primary root seedlings. Analyses was conducted on five independent repetitions. The expression levels were normalized against maize MEP gene and the expression in the -N transition zone samples was set as 1 using $2^{-\Delta\Delta CT}$ method. Data for each region was reported as +N/-N qPCR relative expression values. The bar in red-blue gradation indicates high (red) and low (blue) expression. The responsive transcripts, together with an identifying number (1 to 35) are listed on the left of panel, and the function description on the right.

Fig. 7. Percentage of transcripts distribution in the four different root portions in nitrate-depleted (-N) and in nitrate-supplied (+N) root. Transcripts abundance (%) of the 35 selected transcripts recorded in response to 2h of nitrate supply (+N) or depletion (-N) in each of the four primary root portions (1, meristem enriched zone; 2, transition zone enriched portion; 3 elongation zone enriched portion; 4, maturation zone enriched portion) are reported in the left panel. The right panel shows the increase or decrease (%) in relative transcript abundance obtained by deducing –N (%) to +N (%) values described in the left panel.

Fig. 8. Expression profiles of the selected 35 genes in response to NO_3^-, NO_3^- +tungstate (W) and NO_3^-+cPTIO treatments were assessed by Real time quantitative PCR. qPCR results were reported as relative expression values according to the ratio between W/NO_3^- (black bars) and cPTIO/NO_3^- (grey bars). The expression levels were normalized against maize MEP gene and the expression in the +NO_3^- transition zone enriched samples was set as 1 using $2^{-\Delta\Delta CT}$ method. Error bars represent the standard error of the mean for three biological replicates. Genes were clustered according to their relative expression levels in: down-regulated by both W and cPTIO treatments (A), down regulated by W but up-regulated by cPTIO $^-$ treatments (B), up-regulated by both W and cPTIO treatments (C), up-regulated by W but down-regulated by cPTIO treatments.

Fig. 9. Gene Ontology (GO) term enrichment analysis on proteome data obtained from iTRAQ analysis (Blast2GO software). GO terms of biological process (BP) and molecular function (MF) were analysed and significantly enriched categories (when compared with the entire proteome), FDR $\leq$0.05, were recorded. The percentage of over-represented GO terms among the iTRAQ differentially expressed proteins identified from the comparison between TZ enriched portion of seedlings grown in nitrate supplied or depleted solution are shown. Bars in grey indicate GO terms that are upregulated in the nitrate-supplied tissue *versus* the corresponding control (black bars).

Fig. 10. Proposed model for nitrate response in maize TZ. After nitrate supply, the transcription of a wide set of genes is regulated. This re-programming in transcriptome could be translated in a proteome rearrangement. The transcriptome change could be dependent on both nitrate itself or

on some NR-derived product, as for example the NO, which was confirmed to represent a key signal in the root nitrate response. These molecular events could be implicated in the physiological adaptation of plants to nitrate fluctuations in soil.

Figure 1

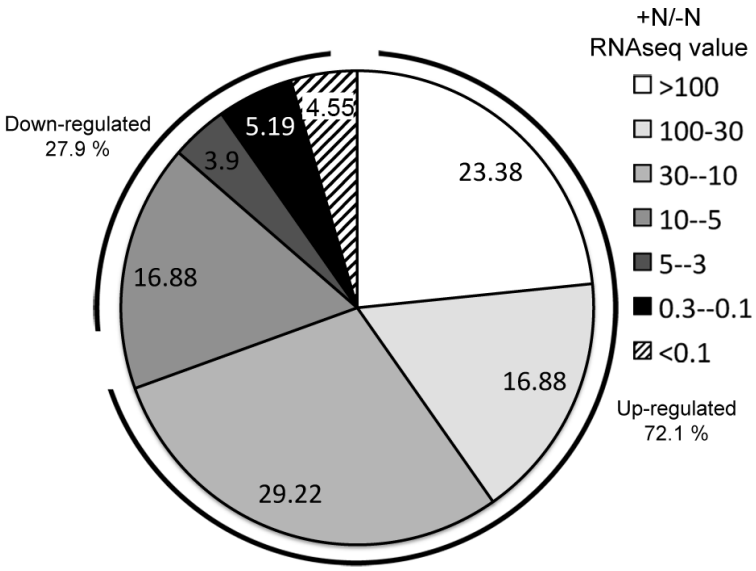
+N/-N
RNAseq value
>100
100-30
30--10
10--5
5--3
0.3--0.1
<0.1
Down-regulated
27.9 %
Up-regulated
72.1 %
23.38
16.88
29.22
16.88
3.9
5.19
4.55

Figure 2

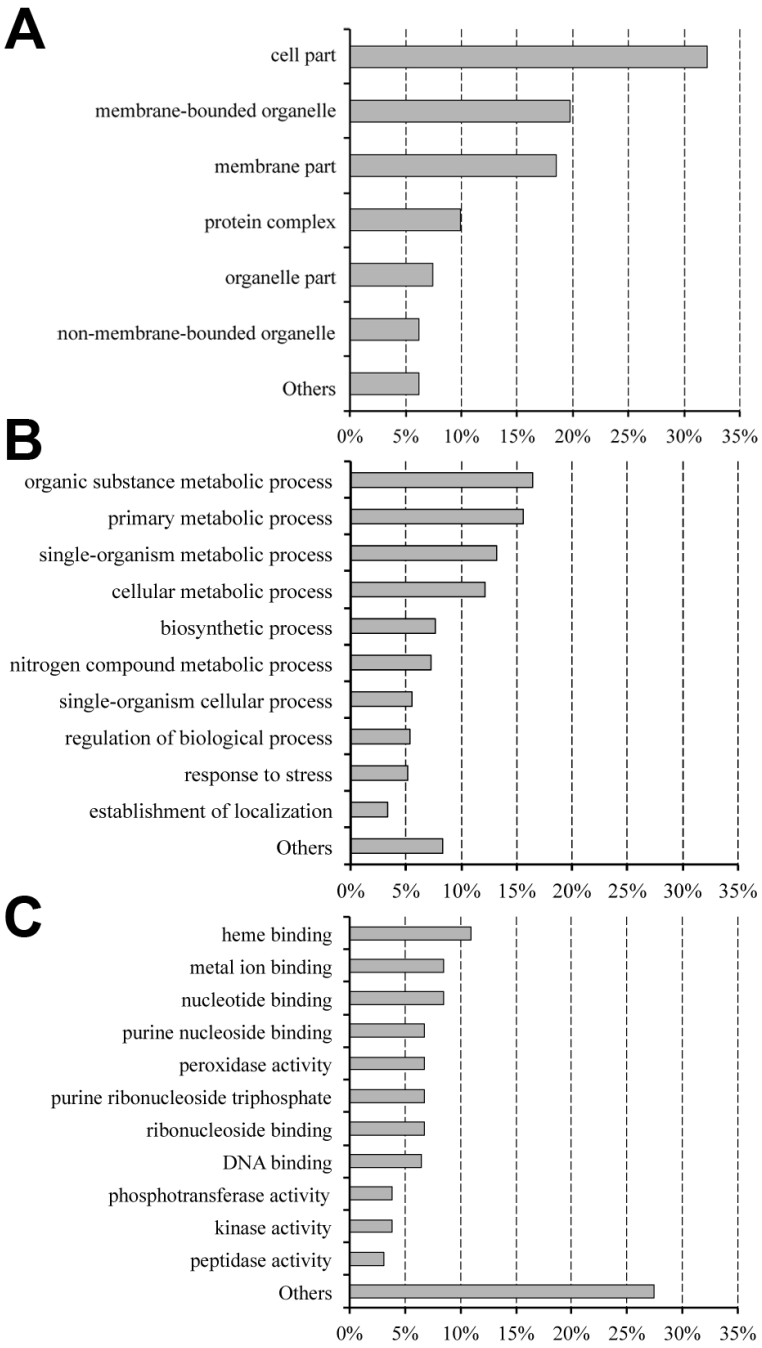
A
cell part
membrane-bounded organelle
membrane part
protein complex
organelle part
non-membrane-bounded organelle
Others
0% 5% 10% 15% 20% 25% 30% 35%
B
organic substance metabolic process
primary metabolic process
single-organism metabolic process
cellular metabolic process
biosynthetic process
nitrogen compound metabolic process
single-organism cellular process
regulation of biological process
response to stress
establishment of localization
Others
0% 5% 10% 15% 20% 25% 30% 35%
C
heme binding
metal ion binding
nucleotide binding
purine nucleoside binding
peroxidase activity
purine ribonucleoside triphosphate
ribonucleoside binding
DNA binding
phosphotransferase activity
kinase activity
peptidase activity
Others
0% 5% 10% 15% 20% 25% 30% 35%

Figure 3

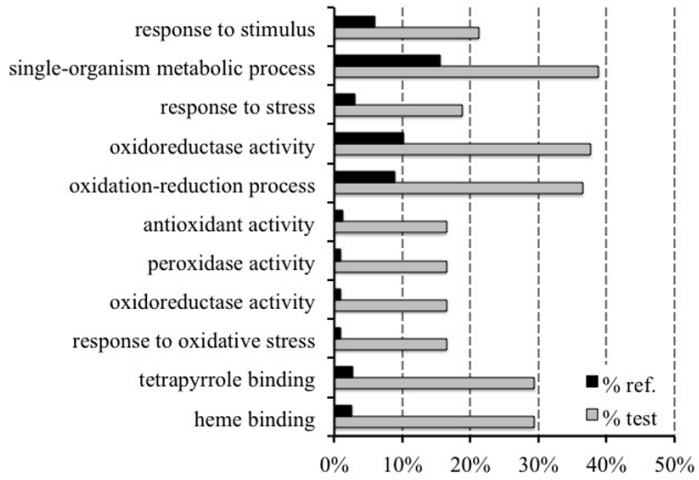

Figure 4

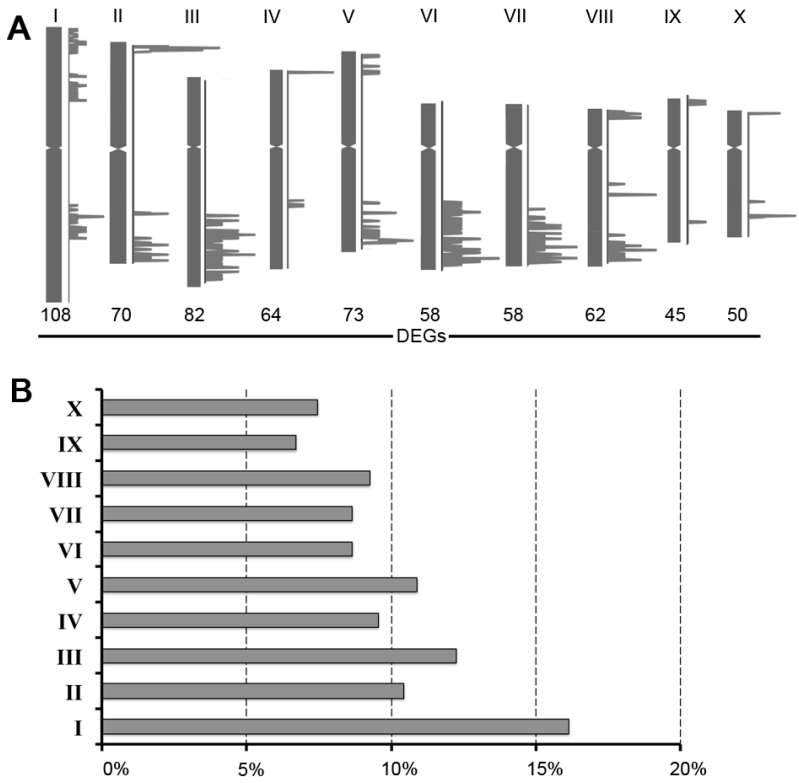

Figure 5

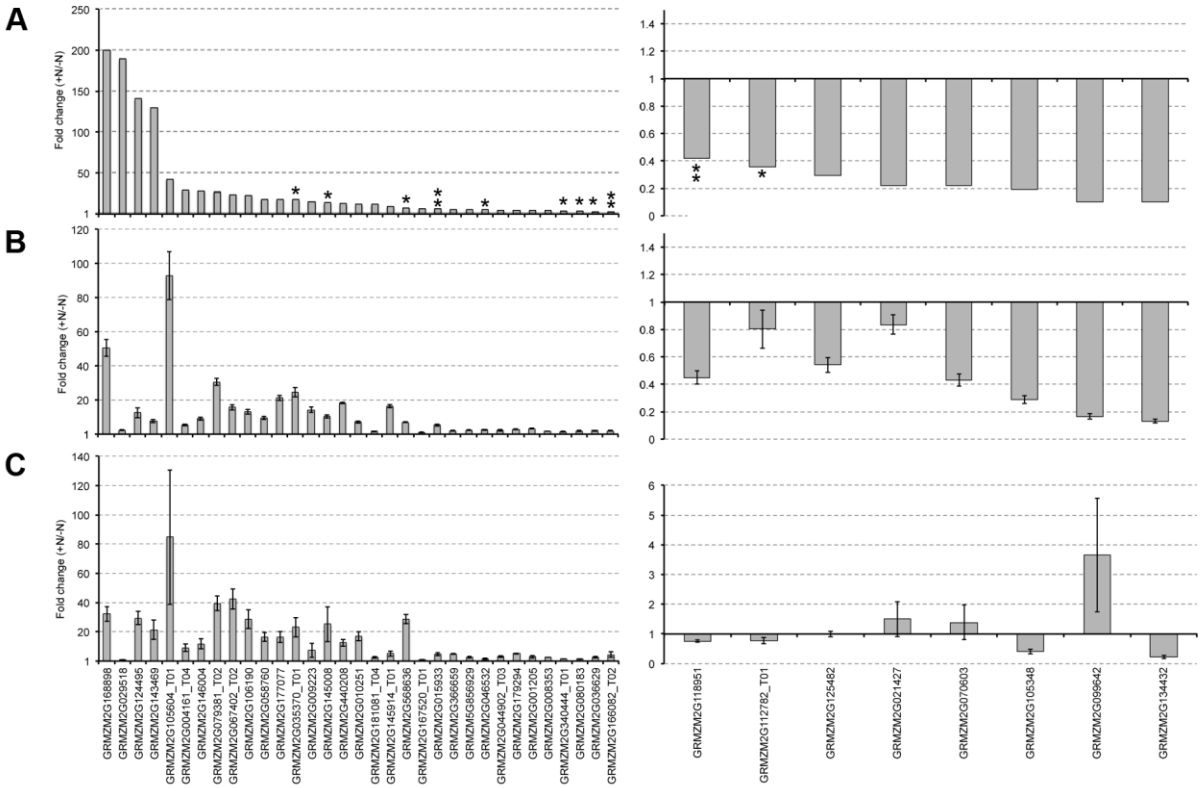
A
B
C
Fold change (+N/-N)
GRMZM2G168898
GRMZM2G029518
GRMZM2G124495
GRMZM2G143469
GRMZM2G105604_T01
GRMZM2G004161_T04
GRMZM2G146004
GRMZM2G079381_T02
GRMZM2G067402_T02
GRMZM2G106190
GRMZM2G058760
GRMZM2G177077
GRMZM2G035370_T01
GRMZM2G009223
GRMZM2G145008
GRMZM2G440208
GRMZM2G010251
GRMZM2G181081_T04
GRMZM2G145914_T01
GRMZM2G568636
GRMZM2G167520_T01
GRMZM2G015933
GRMZM2G366659
GRMZM5G856929
GRMZM2G046532
GRMZM2G044902_T03
GRMZM2G179294
GRMZM2G001205
GRMZM2G009353
GRMZM2G340444_T01
GRMZM2G080183
GRMZM2G036629
GRMZM2G166082_T02
GRMZM2G118951
GRMZM2G112782_T01
GRMZM2G125482
GRMZM2G021427
GRMZM2G070603
GRMZM2G105348
GRMZM2G099642
GRMZM2G134432

Figure 6

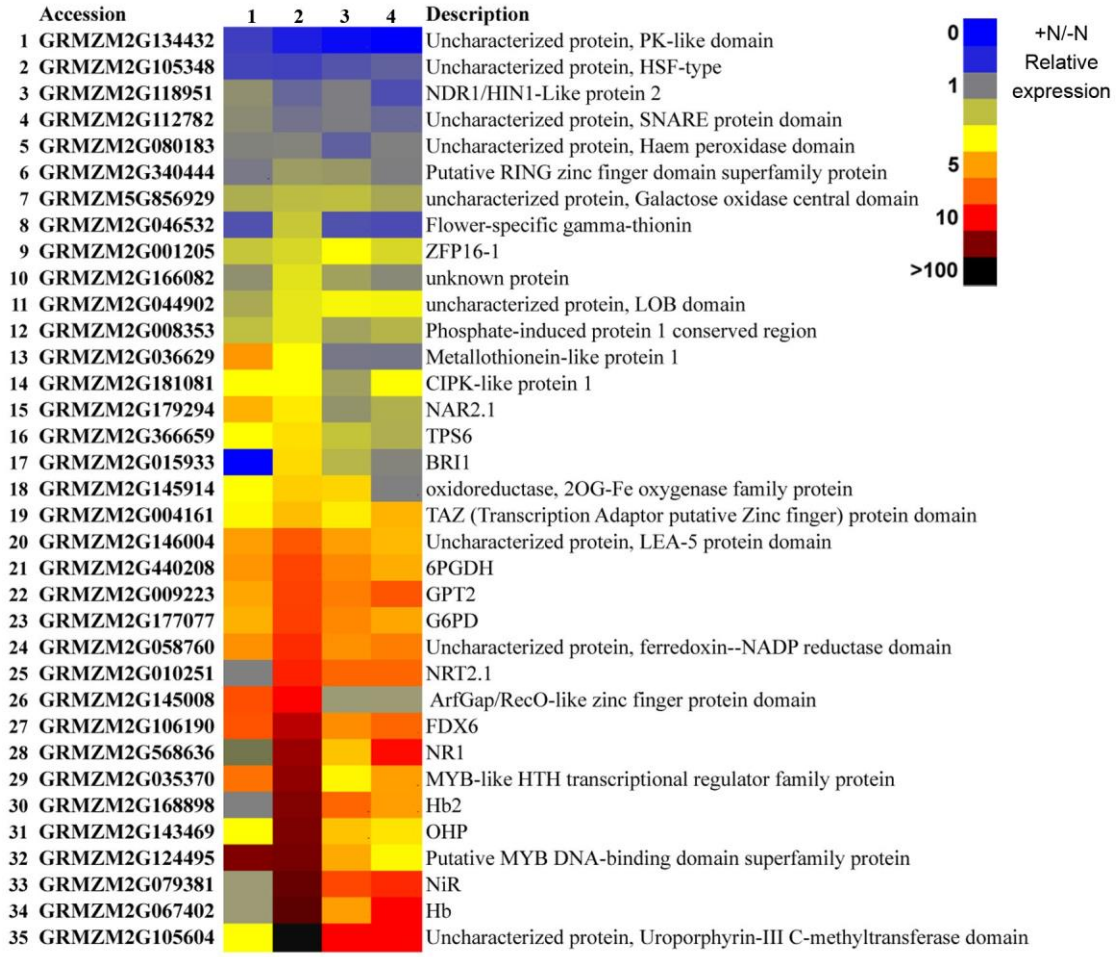
Accession
1
2
3
4
Description
1 GRMZM2G134432 Uncharacterized protein, PK-like domain
2 GRMZM2G105348 Uncharacterized protein, HSF-type
3 GRMZM2G118951 NDR1/HIN1-Like protein 2
4 GRMZM2G112782 Uncharacterized protein, SNARE protein domain
5 GRMZM2G080183 Uncharacterized protein, Haem peroxidase domain
6 GRMZM2G340444 Putative RING zinc finger domain superfamily protein
7 GRMZM5G856929 uncharacterized protein, Galactose oxidase central domain
8 GRMZM2G046532 Flower-specific gamma-thionin
9 GRMZM2G001205 ZFP16-1
10 GRMZM2G166082 unknown protein
11 GRMZM2G044902 uncharacterized protein, LOB domain
12 GRMZM2G008353 Phosphate-induced protein 1 conserved region
13 GRMZM2G036629 Metallothionein-like protein 1
14 GRMZM2G181081 CIPK-like protein 1
15 GRMZM2G179294 NAR2.1
16 GRMZM2G366659 TPS6
17 GRMZM2G015933 BRI1
18 GRMZM2G145914 oxidoreductase, 2OG-Fe oxygenase family protein
19 GRMZM2G004161 TAZ (Transcription Adaptor putative Zinc finger) protein domain
20 GRMZM2G146004 Uncharacterized protein, LEA-5 protein domain
21 GRMZM2G440208 6PGDH
22 GRMZM2G009223 GPT2
23 GRMZM2G177077 G6PD
24 GRMZM2G058760 Uncharacterized protein, ferredoxin--NADP reductase domain
25 GRMZM2G010251 NRT2.1
26 GRMZM2G145008 ArfGap/RecO-like zinc finger protein domain
27 GRMZM2G106190 FDX6
28 GRMZM2G568636 NR1
29 GRMZM2G035370 MYB-like HTH transcriptional regulator family protein
30 GRMZM2G168898 Hb2
31 GRMZM2G143469 OHP
32 GRMZM2G124495 Putative MYB DNA-binding domain superfamily protein
33 GRMZM2G079381 NiR
34 GRMZM2G067402 Hb
35 GRMZM2G105604 Uncharacterized protein, Uroporphyrin-III C-methyltransferase domain
0
1
5
10
>100
+N/-N
Relative
expression

Figure 7

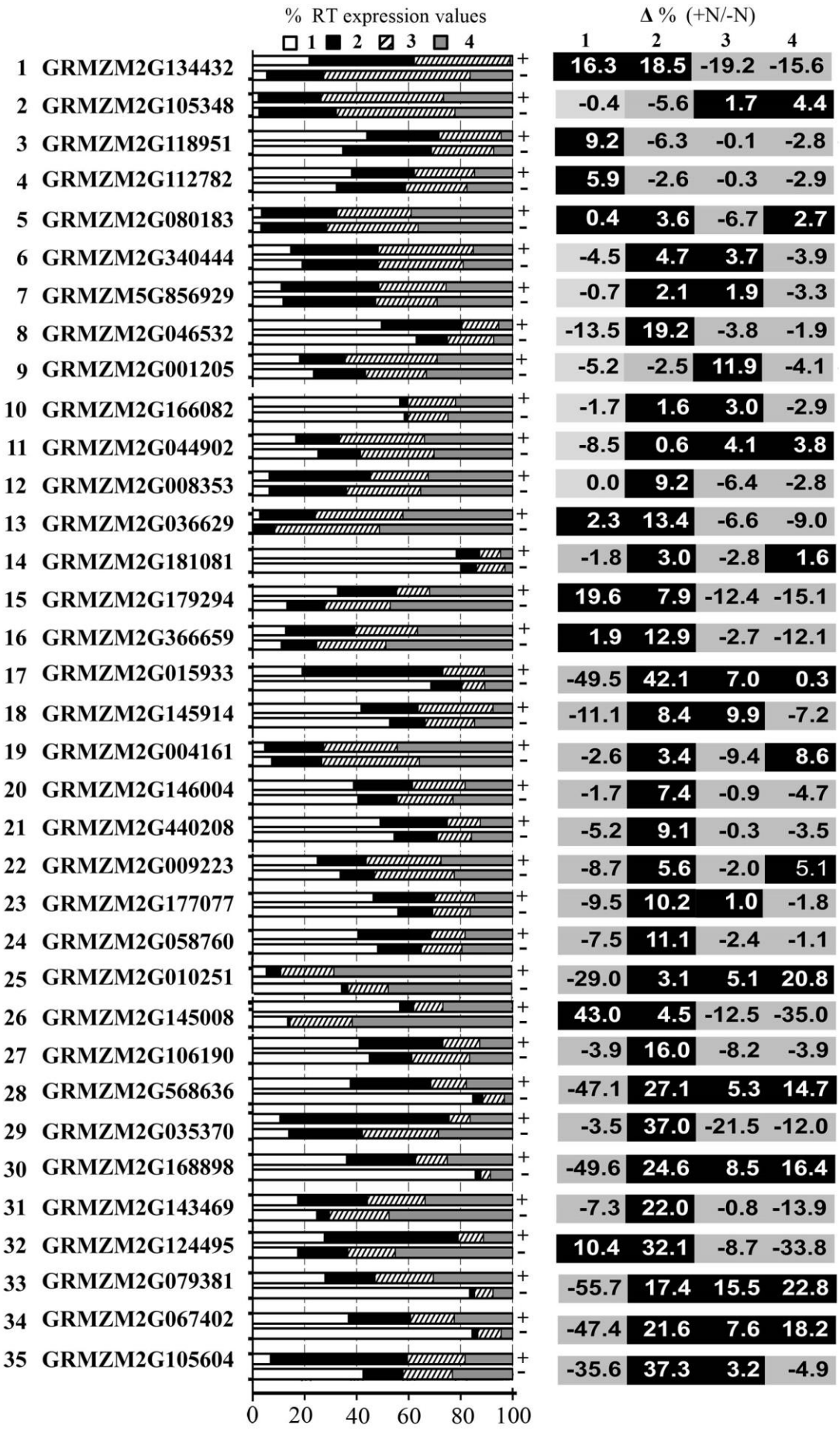
% RT expression values
1 2 3 4
Δ % (+N/-N)
1 2 3 4
1 GRMZM2G134432 16.3 18.5 -19.2 -15.6
2 GRMZM2G105348 -0.4 -5.6 1.7 4.4
3 GRMZM2G118951 9.2 -6.3 -0.1 -2.8
4 GRMZM2G112782 5.9 -2.6 -0.3 -2.9
5 GRMZM2G080183 0.4 3.6 -6.7 2.7
6 GRMZM2G340444 -4.5 4.7 3.7 -3.9
7 GRMZM5G856929 -0.7 2.1 1.9 -3.3
8 GRMZM2G046532 -13.5 19.2 -3.8 -1.9
9 GRMZM2G001205 -5.2 -2.5 11.9 -4.1
10 GRMZM2G166082 -1.7 1.6 3.0 -2.9
11 GRMZM2G044902 -8.5 0.6 4.1 3.8
12 GRMZM2G008353 0.0 9.2 -6.4 -2.8
13 GRMZM2G036629 2.3 13.4 -6.6 -9.0
14 GRMZM2G181081 -1.8 3.0 -2.8 1.6
15 GRMZM2G179294 19.6 7.9 -12.4 -15.1
16 GRMZM2G366659 1.9 12.9 -2.7 -12.1
17 GRMZM2G015933 -49.5 42.1 7.0 0.3
18 GRMZM2G145914 -11.1 8.4 9.9 -7.2
19 GRMZM2G004161 -2.6 3.4 -9.4 8.6
20 GRMZM2G146004 -1.7 7.4 -0.9 -4.7
21 GRMZM2G440208 -5.2 9.1 -0.3 -3.5
22 GRMZM2G009223 -8.7 5.6 -2.0 5.1
23 GRMZM2G177077 -9.5 10.2 1.0 -1.8
24 GRMZM2G058760 -7.5 11.1 -2.4 -1.1
25 GRMZM2G010251 -29.0 3.1 5.1 20.8
26 GRMZM2G145008 43.0 4.5 -12.5 -35.0
27 GRMZM2G106190 -3.9 16.0 -8.2 -3.9
28 GRMZM2G568636 -47.1 27.1 5.3 14.7
29 GRMZM2G035370 -3.5 37.0 -21.5 -12.0
30 GRMZM2G168898 -49.6 24.6 8.5 16.4
31 GRMZM2G143469 -7.3 22.0 -0.8 -13.9
32 GRMZM2G124495 10.4 32.1 -8.7 -33.8
33 GRMZM2G079381 -55.7 17.4 15.5 22.8
34 GRMZM2G067402 -47.4 21.6 7.6 18.2
35 GRMZM2G105604 -35.6 37.3 3.2 -4.9
+
-
0 20 40 60 80 100

Figure 8

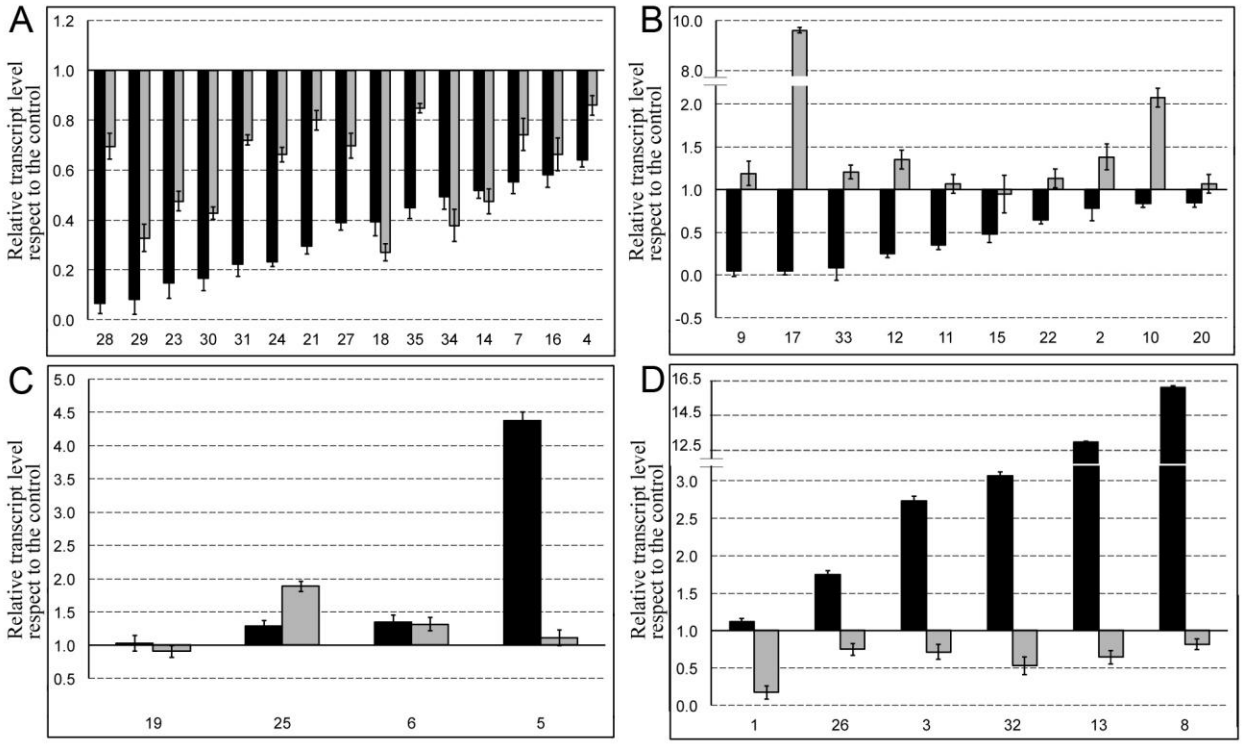

Figure 9

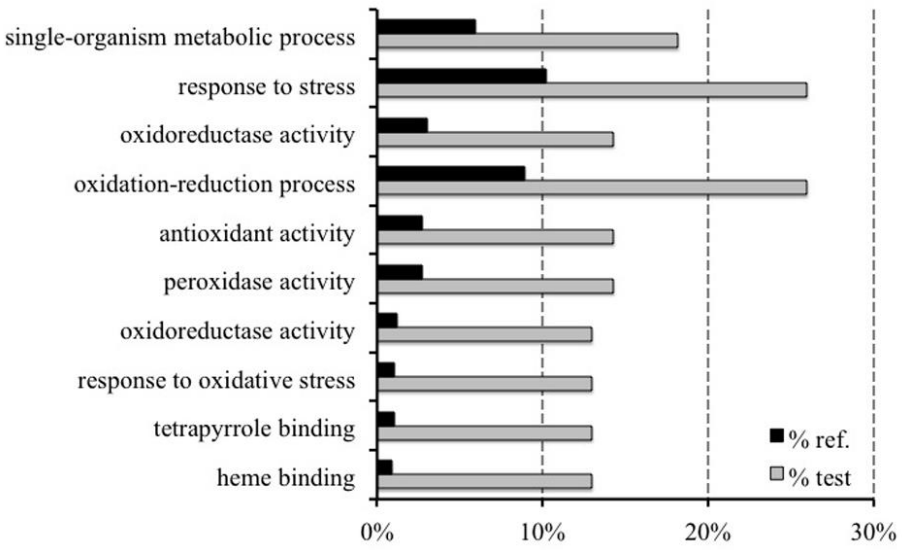

Figure 10

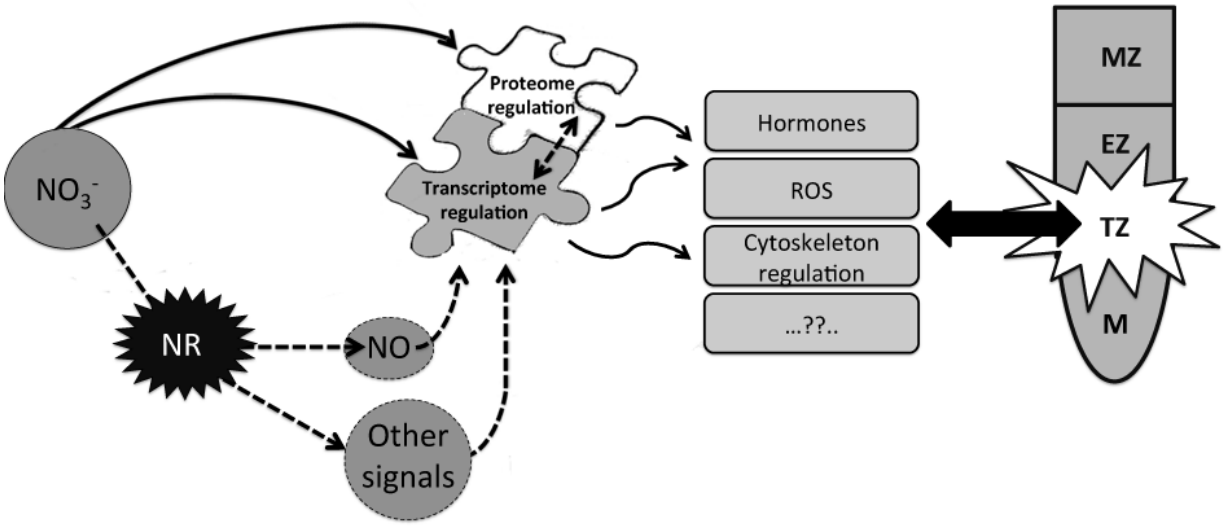
Proteome regulation
Transcriptome regulation
NO_3^-
NR
NO
Other signals
Hormones
ROS
Cytoskeleton regulation
...??..
MZ
EZ
TZ
M